KLF4 regulates trophoblast function and associates with unexplained recurrent spontaneous abortion

Yiling Tan[1†], Jiayu Wang[1†], Chunming Liu[3†], Shujuan Wu[4], Mengqi Zhou[1], Yan Zhang[2*], Tailang Yin[1*] and Jing Yang[1*]

Abstract

Background Recurrent spontaneous abortion (RSA) is defined as two or more consecutive spontaneous abortions before 20 weeks with the same spouse [1]. However, approximately 50% of RSA cases of unknown cause are classified as unexplained recurrent spontaneous abortion (URSA). Potential factors include decreased trophoblast cell migration and invasion, leading to impaired placental implantation and maintenance of the normal maternal-fetal interface. However, the mechanism of this pathogenesis remains unknown. In this study, we investigated the potential role and mechanism of KLF4 in regulating URSA by influencing the invasion and migration ability of trophoblast cells.

Methods We firstly identified 817 differentially expressed genes by performing a difference analysis of the dataset GSE121950 [2] related to recurrent abortion, and intersected the top 10 genes obtained respectively by the three algorithms: DMNC, MNC, and EPC using Venn Diagram. To detect the expression levels of core genes, villi samples were obtained from normal pregnant women and patients with URSA. RT-qPCR analysis revealed a significant difference in KLF4 mRNA expression and KLF4 was then analyzed. Trophoblast cell lines HTR8 and JEG3 were used to investigate the effect of KLF4 on trophoblastic function. Wound healing and transwell assays was performed to detect the invasion and migration of trophoblast cells. The expression of epithelial-mesenchymal transition(EMT) molecules were detected by RT-qPCR and western blot. Promoter detection and epigenetic modification were detected by chromatin immunoprecipitation (ChIP) assay. Molecular nuclear localization was detected by immunofluorescence and subcellular fractionation. Miscarried mice model was used to study the effects of KLF4 on URSA induced by reduced trophoblast invasion and migration.

Results KLF4 is highly expressed in the villi of patients with URSA. KLF4 inhibits the expression level of H3R2ME2a in trophoblast cells by regulating the transcriptional level and nuclear translocation of PRMT6, thereby inhibiting the possible regulatory mechanism of trophoblastic invasion and providing a potential treatment strategy for URSA in vivo.

†Yiling Tan, Jiayu Wang and Chunming Liu have contributed equally to this work.

*Correspondence:
Yan Zhang
peneyyan@whu.edu.cn
Tailang Yin
reproductive@whu.edu.cn
Jing Yang
dryangjing@whu.edu.cn
Full list of author information is available at the end of the article

Tan *et al. Journal of Translational Medicine*   (2024) 22:922

Page 2 of 25

Conclusions The KLF4/PRMT6/H3R2ME2a axis regulates mechanisms associated with unexplained recurrent spontaneous abortion by regulating trophoblast function.

Highlights

1. KLF4 is highly expressed in the villi of patients with URSA.
2. KLF4 inhibits trophoblast function by inhibiting PRMT6 expression.
3. KLF4 inhibits trophoblast function by inhibiting the transcription and nucleation of PRMT6, thereby inhibiting the expression of H3R2ME2a.

Keywords KLF4, Unexplained recurrent spontaneous abortion, PRMT6, H3R2ME2a, Trophoblast invasion

Introduction

Recurrent spontaneous abortion (RSA), defined as two or more consecutive spontaneous abortions before 20 weeks, affects 2–5% of reproductive women globally [3]. The causes include anatomical structure and chromosomal abnormalities, genetic factors, endocrine abnormalities, and immune dysfunction [4]. However, approximately 50% of RSA cases of unknown cause are classified as unexplained recurrent spontaneous abortion (URSA). This not only affects the physical and mental health of the majority of pregnant women but also imposes a substantial burden and mental pressure on their families and society. Embryo development primarily depends on the placenta tissue formed after blastocyst implantation to provide nutrition. Placental formation begins when trophoblast cells enter the uterus at the maternal-fetal interface between the uterine mucosa and ectoderm, allowing direct contact between trophoblasts and maternal blood for nutrient and metabolite exchange. Incomplete placental formation and abnormal maternal-fetal interface in early pregnancy are considered potential causes of URSA [3]. In early pregnancy, trophoblast cells showed high invasion and migration ability like malignant tumor cells; however, they were abnormally reduced under pathological conditions, suggesting that appropriate invasion and migration ability of trophoblast is essential for early embryo implantation and placental development and for establishing proper maternal-fetal relationship [4]. Epithelial-mesenchymal transformation (EMT) is characterized by the loss of adhesive epithelial phenotype and acquisition of active mesenchymal phenotype, significantly promoting migration and invasion of extravillous trophoblast cells [5]. Impaired invasion and migration of trophoblast cells due to EMT obstruction may increase URSA [6]; however, the underlying molecular mechanism remains unclear.

KLF4 is a member of the evolutionarily conserved family of zinc finger transcription factors, also known as epithelial zinc finger protein (EZF) and gut-enriched Krüppel-like factor (GKLF). KLF4 may act as an oncogene in different tumor tissues, and its biological behavior is regulated by different molecular mechanisms [7]. For example, KLF4 can inhibit the invasion of thyroid tumors by inhibiting the expression of MMP2 and MMP9 [8]. De-ubiquitination of KLF4 can inhibit its self-degradation and increase the incidence of lung adenocarcinoma [9]. Based on these results and the tumor similarity of placental trophoblast cells, KLF4 may be linked to trophoblastic function and play an important role at the maternal-fetal interface. However, the potential role of KLF4 in URSA and its specific mechanism of action remain unclear.

Histones are basic proteins that bind to DNA. As core components, they form nucleosome structures with 147 bp DNA fragments wrapped around them, forming octamers containing four core histones (H3, H4, H2A, and H2B). Each protein, primarily a globohistone, has a characteristic side chain or tail that is densely packed with alkaline lysine and arginine residues and is capable of covalent post-translational modifications (PTM) at different amino acid sites, including acetylation, methylation, phosphorylation, ubiquitination, and SUMO. These modifications control the chromatin state by altering the charge density between histones and DNA, affecting chromatin organization and potentially transcription processes [10]. These PTMs can also serve as recognition blocks for specific binding proteins that, when bound, may signal changes in chromatin structure or function and play important roles in various biological processes, including gene epigenetic regulation, DNA repair, mitosis, and meiosis. Histone modification has been shown to affect the genesis and development of tumors by affecting the expression of oncogenes or tumor suppressor genes as well as changes in the metabolic pathway of tumor cells [11], thereby affecting the biological process of the malignant degree of tumor cells [12].

Tan *et al. Journal of Translational Medicine*   (2024) 22:922

Page 3 of 25

Furthermore, histone modification may be an important target in regulating placental growth and development and its invasion of the maternal uterus. MAP3K4-mediated histone acetylation regulates the epithelial-mesenchymal transition process in mouse trophoblast stem cells [13]. Moreover, the level of acetylated histone (H3) is decreased during the differentiation of cytotrophoblasts in vitro [14]. During human trophoblast syncytialization, H3K9ME3 of ERG3, cFOS, and cJUN transcription factors increased, while H3K27AC and H3K9AC decreased, accompanied by increased histone deacetylase activity. Histone modification is also involved in the molecular biological process of ectrophoblast cells in a pathological state. During preeclampsia, the fourth lysine trimethylation (H3K4me3) and ninth lysine acetylation (H3K9AC) levels of histone H3 in villus trophoblast cells of the placenta decreased, and the invasion and migration of trophoblast cells were affected by the PPARγ activity [15]. It has also been confirmed that histone lactate levels are increased in preeclampsia, possibly due to trophoblast cell hypoxia, thereby promoting fibrosis-related gene expression and providing new insights into the mechanism of histone modification in placental dysfunction during preeclampsia [16]. Changing histone modification of trophoblast cells has become an important target in regulating the EMT, invasion, and migration abilities of trophoblast cells. The regulation of URSA by histone modification of exovillous trophoblast cells and its mechanism remains unknown. Therefore, a comprehensive investigation of the molecular mechanism of histone modification in extravillous trophoblast cells might provide a strong theoretical basis for the diagnosis and treatment of URSA.

Trophoblasts exhibit high EMT, invasion, and migration abilities during early pregnancy. Therefore, we hypothesized that histone modifications may play an important role in regulating trophoblast characteristics. The transcriptome of villus tissue of URSA patients was analyzed in the database, and the differentially expressed gene KLF4 was screened out. We discovered that KLF4 can regulate the asymmetric methylation modification of arginine residues at the H3R2 site of histone by mediating the protein arginine methyltransferase (PRMT6), thereby causing dysregulation of H3R2ME2a level, leading to URSA.

Results

KLF4 expression is upregulated in the villus tissue of URSA patients and the placenta of miscarried mice

By performing a difference analysis of the dataset GSE121950 [17] related to recurrent abortion, 817 differentially expressed genes were identified in the villi tissues of the URSA group compared to the normal pregnancy (NP) group, of which 460 were upregulated, and 357 were downregulated. The threshold values of |log2FC|> 1 and $p < 0.05$ were shown on the volcano map (Fig. 1A), while the top 100 genes are illustrated on the heat map (Fig. 1B). Next, GO and KEGG enrichment analyses were performed on differentially expressed genes (Figs. S1A-D). GO analysis revealed that the NP and the URSA groups differed primarily in interferon release, ERK1/2 signal activation, cell progression, and metabolic processes. KEGG analysis showed that different genes were primarily enriched in the HIF-1a signaling, EGFR, and other signaling pathways.

To screen for core genes, the STRING website was used for protein interaction analysis and visualization of the interaction network (Fig. S1E). To further screen the core submodules, topologica l algorithm analysis was performed using three algorithms: DMNC, MNC, and EPC (Fig. 1C–E). The intersection of the top 10 genes obtained by the three algorithms was determined using Venn Diagram (Fig. F), and the last seven core genes were screened out: ALDH1A1, KLF4, KRT5, ATF2, MEF2A, SOX9, and UBE2I.

(See figure on next page.)

Fig. 1 KLF4 expression is up-regulated in the villus tissue of URSA patients and placenta of miscarried mice. **A** Volcano plots showed significantly different expression genes of villus in normal pregnant women ($n = 3$) and URSA pregnant women ($n = 3$) in dataset GSE121950.The screening condition was set as Ilog2FCI> 1 and P value < 0.05. **B** The heat map shows the top 100 genes with the most significant differences. **C–E** Three algorithms, DMNC, MNC and EPC, were used to analyze the topology algorithm of the different genes. **F** The top ten genes obtained by the three algorithms are intersected by the Venn diagram, and 7 core genes are obtained. **G** The mRNA expression of 7 core genes in villus tissues of normal pregnant women ($n = 20$) and URSA pregnant women ($n = 12$) were detected by qPCR. **H** The expression of KLF4 protein in chorionic villus of normal pregnancy patients ($n = 7$) and URSA patients ($n = 7$) was determined by western blot. The protein imprinting strength was quantified using ImageJ software. **I** The expressions of KLF4 protein in villi of normal pregnancy patients ($n = 3$) and URSA patients ($n = 3$) were determined by immunofluorescence. The fluorescence staining intensity was quantified by ImageJ software. **J** Representative immunofluorescence images: double immune-staining of CK7 (red) and KLF4 (green); double immune-staining of HLA-G (red) and KLF4 (green) **K** The embryo absorption rate of normal pregnancy (NP) and aborted pregnancy (AP) mice at day 13.5 of gestation was calculated, which was defined as the number of resorbed embryos / (number of resorbed embryos + number of fetuses surviving) × 100%. **L–N** In NP group ($n = 4$) and AP group ($n = 4$), the expression of KLF4 was determined by qPCR, western blot and immunohistochemistry of placental tissue sections. ImageJ software was used to quantitatively analyze the imprinting strength and the relative absorbance of immunohistochemistry

Fig. 1 (See legend on previous page.)

Tan *et al. Journal of Translational Medicine*   (2024) 22:922

Page 5 of 25

To detect the expression levels of core genes, villi samples were obtained from normal pregnant women and patients with URSA. RT-qPCR analysis revealed a significant difference in KLF4 mRNA expression (Fig. 1G). KLF4 was then analyzed. Western blot analysis showed that the protein content of KLF4 was significantly increased in the villus tissues of URSA patients (Fig. 1H). To verify these results, the expression of KLF4 in villi tissue sections of NP and URSA patients was compared using immunofluorescence staining (Fig. 1I). Stronger expression of KLF4 was observed in tissue of the URSA group, with the positive cells mainly being cytotrophoblasts and EVTs. To verify the above result, we respectively used immunofluorescence staining with antibodies of CK7 as a marker of cytotrophoblasts, and HLA-G, as a marker of EVTs on human villous tissue (Fig. 1J). Immunofluorescence shows resemblant results. These results showed that KLF4 expression was increased in the villi of URSA patients compared to healthy controls, confirming the differential expression. Moreover, mouse models of NP and abortion-prone pregnancy (AP) were constructed. The results showed that the embryo absorption rate in the AP group increased significantly (Fig. 1K). The expression of KLF4 in mouse placenta was determined using qPCR, western blot, and IHC (Fig. 1L-N). The results revealed that the placenta of the AP mice exhibited increased expression of KLF4 compared to the NP mice. These results indicate that KLF4 was significantly upregulated in the villus tissue of URSA patients and placental tissue of aborted mice; therefore, KLF4 may be involved in the pathological process of URSA.

KLF4 inhibits trophoblast migration, invasion, and epithelial-mesenchymal transformation(EMT)

To explore the potential role of KLF4 in the pathogenesis of URSA, the STRING website was used to conduct interaction analysis of KLF4 and the signature proteins of proliferation, invasion, migration, apoptosis, and EMT, and found that KLF4 was significantly associated with EMT and proteins related to invasion and migration (Fig. S2A). Next, the effects of KLF4 on trophoblast cell invasion, migration, and EMT behavior were investigated. First, we used the HTR8 and JEG3 cell lines to construct KLF4 stable knockdown and overexpressed cell lines, respectively, and detected the expression of invasion and migration marker gene MMP9 by measuring mRNA and protein levels (Fig. 2A-D). The results revealed that MMP9 expression increased in KLF4 knockdown trophoblast cell lines while it decreased in KLF4 overexpressed cells. To further analyze the migration and invasion abilities of HTR8 and JEG-3 cells, wound healing and transwell assays were performed. The results indicated that KLF4 overexpression reduced trophoblast migration and invasion, whereas KLF4 knockdown improved these abilities (Fig. 2E-H).We detected the expression levels of EMT-related proteins E-cadherin, N-cadherin and vimentin in trophoblast cell lines, and observed that the expression of E-cadherin increased in the overexpressed group, while the expression of N-cadherin and vimentin decreased (Figs. 2I-L). The knockdown group showed the opposite result, suggesting that KLF4 inhibits EMT of the trophoblast.

KLF4 inhibits PRMT6 transcription and nuclear translocation

We respectively performed karyoplasmic separation experiments on HTR8 and JEG3 cell lines to determine the underlying mechanism of KLF4 in trophoblast cells. The results revealed that KLF4 was localized in the nucleus (Fig. 3A, B). Immunofluorescence revealed a significant association between KLF4 expression and nuclear localization (Fig. 3C, D), which confirmed this conclusion. We speculate that KLF4 may function as a transcription factor in trophoblast cells. Moreover, differentially expressed genes were analyzed in HTR8 cells of the control and KLF4 knockdown groups using RNA-seq. According to the threshold value of |log2FC|> 0.75 and *P* < 0.05, 915 significant differentially expressed genes were evaluated, among which 213 genes were upregulated, and 702 genes were downregulated (Fig. 3E). The significant differential genes were displayed using a heat map (Fig. 3F). Among these, transcriptional differences in the protein arginine methyltransferase (PRMT) family attracted our interest. Arginine methyltransferase-mediated arginine methylation is a common post-translational modification (PTM) in many proteins, involved in gene expression, mRNA processing and translation, transcription and post-transcriptional regulation, intracellular signaling, and in the development and progression of many diseases, especially tumors [18]. The PRMT family includes PRMT1-9, of which PRMT6 showed the most significant changes in mRNA levels in KLF4 knockdown trophoblast cell lines (Fig. 3F, G). PRMT6 can affect cell growth, migration, invasion, apoptosis, and other biological behaviors in various cancers, making it a potential antitumor therapeutic target [19].

Based on the biological behavior similarity between trophoblast cells and various tumor cells, PRMT6 may play a similar role. Therefore, PRMT6 expression was further analyzed. Western blot revealed that the PRMT6 gene was down-regulated in the KLF4 over-expressing group and upregulated in the KLF4 knockdown group in both trophoblast cell lines (Fig. 3H, I). Next, we constructed stable knockdown and overexpressed PRMT6 cell lines using HTR8 and JEG3 cell lines and measured the expression levels of invasion
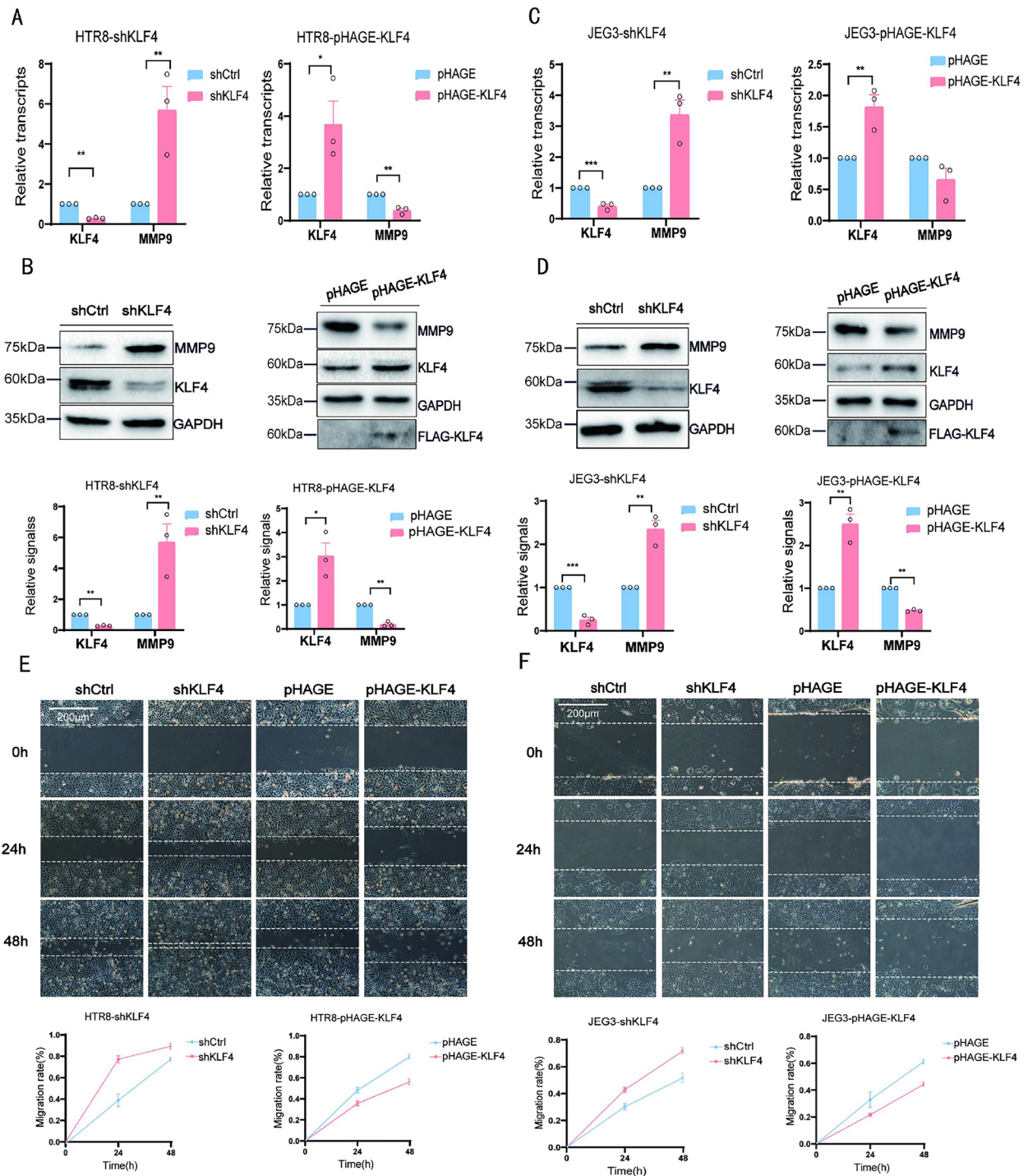
Tan *et al. Journal of Translational Medicine*   (2024) 22:922

Page 6 of 25

Fig. 2 KLF4 inhibits trophoblast migration, invasion, and epithelial-mesenchymal transformation(EMT) **A**–**E** HTR8 and JEG3 cell lines with stable knocked down or overexpression of KLF4 were constructed, and the levels of invasion and migration marker MMP9 were determined by qPCR and western blot, and the imprinting strength of the protein was quantitatively analyzed by ImageJ software. **E**, **F** Wound healing scratches were imaged immediately, 24 h and 48 h after initial scratch time to quantify relative migration, quantifying relative migration using ImageJ software. **G**, **H** HTR8 cells and JEG3 cells were suspended in serum-free medium and then inoculated into an insertion chamber pre-coated with diluted matrix gel and incubated for 48 h for invasion determination. Cells at the lower surface of the membrane were counted and analyzed under a light microscope in three random fields of view. The staining intensity was quantified using the ImageJ software. **I**, **L** The expression levels of E-cadherin, N-cadherin and vimentin markers of epithelial mesenchymal transformation in trophoblast cells with knockdown or overexpression of KLF4 were measured by qPCR and western blot, and the imprinting strength of proteins was quantitatively analyzed by ImageJ software
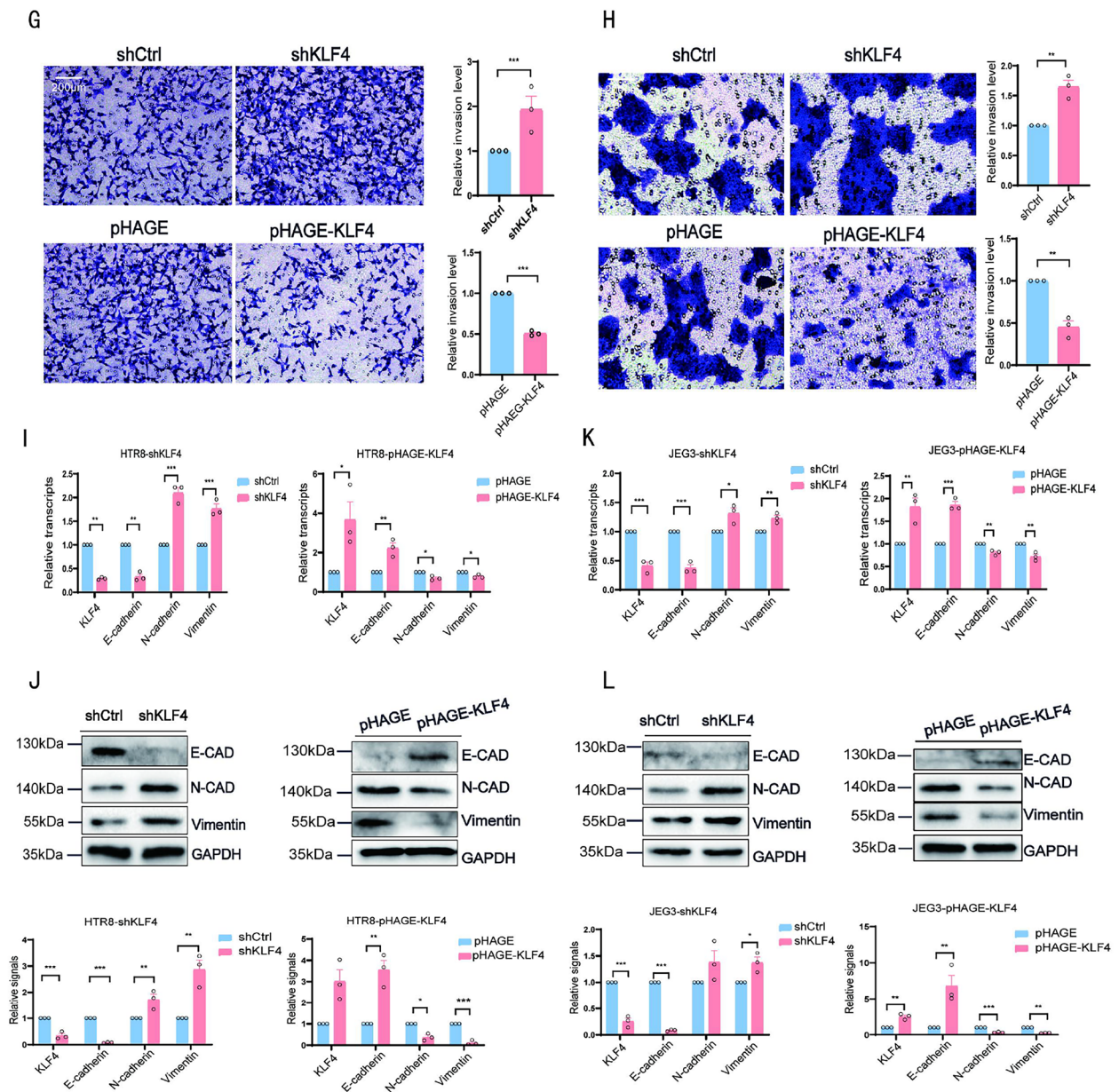
Tan *et al. Journal of Translational Medicine*   (2024) 22:922

Page 7 of 25

Fig. 2 continued

and migration marker gene MMP9 at mRNA and protein levels (Fig. 3J–M). The results revealed that MMP9 expression decreased in PRMT6 knockdown trophoblast cell lines, while it increased in PRMT6 overexpressed cells. The results of wound healing and transwell assays performed on PRMT6 knockdown and overexpressed HTR8 and JEG-3 cells revealed that PRMT6 promoted trophoblast migration and invasion. We measured the expression levels of EMT-related proteins E-cadherin, N-cadherin, and vimentin in trophoblast cell lines and observed that the expression of E-cadherin decreased in the overexpression group, whereas that of N-cadherin and vimentin increased. The knockdown group showed the opposite result, suggesting that PRMT6 promoted EMT of the trophoblast (Fig. 3R–U). However, the mechanism through which KLF4 regulates PRMT6 transcription and function remains unclear. Chromatin co-immunoprecipitation (ChIP) assay revealed that KLF4 was significantly enriched in the PRMT6 transcriptional promoter sequence (Fig. 3V). The specific binding sites for −1806 - −1795 were predicted using the IBS2.0 and JASPAR database (https://jaspar.genereg.net/) (Fig. 3W).

Tan *et al. Journal of Translational Medicine*   (2024) 22:922

Page 8 of 25

Moreover, karyoplasmic separation was conducted on HTR8 cells, and the expression of PRMT6 in different cell components was detected using western blot. The results revealed that KLF4 knockdown promoted the entry of PRMT6 into the nucleus, while KLF4 overexpression inhibited it (Fig. 3X). Immunofluorescence staining confirmed this conclusion (Fig. 3Y). These results indicate that KLF4 can regulate PRMT6 expression by binding to the PRMT6 promoter sequence and inhibit its entry into the nucleus to perform a function. PRMT6 can promote trophoblast cell invasion, migration, EMT, and other biological behaviors.qPCR and western blot were used to determine PRMT6 expression in the placental villi of normal pregnant women and URSA patients. The mRNA and protein levels of PRMT6 were decreased in the villi tissues of URSA patients (Fig. 3Z-AB). To verify these results, triple immunofluorescence staining was used to compare PRMT6 expression in the villous tissue sections of URSA patients and normal pregnant women, as well as co-stained KLF4. The results revealed that PRMT6 expression was lower in URSA patients than in the normal control group, confirming the differential expression (Fig. 3AC). Using multiple immunofluorescence staining and quantitative analysis of fluorescence intensity, we discovered that the expression of PRMT6 and KLF4 was negatively correlated in villi tissues (Fig. 3AD). Moreover, PRMT6 expression at the placental interface in NP and AP mice was determined using qPCR, western blot, and IHC.

The expression of PRMT6 at the placental interface was lower in AP mice than in NP mice (Fig. 3AE–AG). These findings indicate that PRMT6 was significantly downregulated in URSA female villi tissue and placenta tissue of aborted mice. Moreover, PRMT6 may be involved in the KLF4-mediated pathological process of URSA, although the specific mechanism has not been elucidated.

PRMT6 inhibited the level of asymmetric methylation of arginine at the histone H3R2 site

PRMT6 can asymmetrically methylate arginine residues at the histone H3R2 site in a variety of cell lines, thereby mediating the invasion, migration, and other biological behaviors of tumor cells [20]. We first detected the asymmetric methylation level of arginine at the histone H3R2 site (H3R2ME2a) in PRMT6 overexpressed and knockdown trophoblast cell lines. H3R2ME2a levels decreased in PRMT6 knockdown trophoblast cells and increased in cells overexpressing PRMT6 (Fig. 4A, B). These results confirm that PRMT6 can regulate H3R2ME2a levels. We created a mutant trophoblast cell line at the H3R2

(See figure on next page.)

Fig. 3 KLF4 inhibited PRMT6 transcription and nuclear translocation. **A**, **B** Western blot was performed to compare the levels of KLF4 in the nucleus and cytoplasm. Histone H3 was used as a nuclear marker and GAPDH was used as a cytoplasmic marker. **C**, **D** HTR8 and JEG3 cells were inoculated on cell slides for immunofluorescence staining, with KLF4 in red and DAPI in blue, to evaluate the subcellular localization of KLF4. The images were taken with a Zeiss confocal microscope at 40x. **E** Total RNA was isolated from control and KLF4 knockdown HTR8 cells, and RNA-seq analysis was performed. The threshold Ilog2FCI>0.75 and P value < 0.05 were used to display the differentially significant genes on volcano map. **F** Heat maps showing genes with significant differences. **G** The expression of PRMT family 1–9 in HTR8 cells with KLF4 knockdown was analyzed by qPCR. **H**, **I** The protein expression level of PRMT6 in trophoblast cell lines with knockdown and overexpression of KLF4 was determined by western blot. **J**–**M** HTR8 and JEG3 cell lines with stable knocked down or overexpression of PRMT6 were constructed, and the levels of invasion and migration marker MMP9 were determined by qPCR and western blot. The protein imprinting strength was quantitatively analyzed by ImageJ software. **N**, **O** Wound healing scratches were imaged immediately, 24 h and 48 h after initial scratch time to quantify relative migration, quantifying relative migration using ImageJ software. **P**, **Q** HTR8 cells and JEG3 cells were suspended in serum-free medium and then inoculated into an insertion chamber pre-coated with diluted matrix gel and incubated for 48 h for invasion determination. Cells at the lower surface of the membrane were counted and analyzed under a light microscope in three random fields of view. The staining intensity was quantified using the ImageJ software. **R–U** The expression levels of E-cadherin, N-cadherin and vimentin markers of epithelial mesenchymal transformation in trophoblast cells with PRMT6 knockdown or overexpression were determined by qPCR and western blot. The imprinting strength of proteins was quantitatively analyzed by ImageJ software. **V** The KLF4 occupancy of PRMT6 promoter in HTR8 cells of control group and PRMT6 overexpression group was analyzed by ChIP-qPCR. **W** Predicting KLF4 in PRMT6 promoter specific binding sites for − 1806~-1795 by IBS2.0 and JASPAR database (https://jaspar.genereg.net/)(Table S4). **X** Karyoplasmic separation experiments were performed on HTR8 cell lines with KLF4 knockdown and KLF4 overexpression respectively. Histone H3 was used as a nuclear marker and GAPDH was used as a cytoplasmic marker by protein immunoimprinting to detect the expression of PRMT6 in each cell component. **Y** HTR8 cell lines were inoculated on cell slides for immunofluorescence staining, with PRMT6 in red and DAPI in blue, to evaluate the subcellular localization of PRMT6. The images were taken with a Zeiss confocal microscope at 40x. **Z** The mRNA expression of PRMT6 in villus tissues of normal pregnant women ($n = 20$) and URSA pregnant women ($n = 12$) were detected by qPCR.(AB)The expression of PRMT6 protein in chorionic villus of normal pregnancy patients ($n = 7$) and URSA patients ($n = 7$) was determined by western blot. The protein imprinting strength was quantified using ImageJ software.(AC) The expressions of PRMT6(pink) protein and KLF4(green) protein in villi of normal pregnancy patients ($n = 3$) and URSA patients ($n = 3$) were determined by immunofluorescence. The fluorescence staining intensity was quantified by ImageJ software.(AD)The correlation between PRMT6 and KLF4 protein expression levels was calculated by correlation analysis of immunofluorescence staining intensity in tissue sections.(AE-AG)In NP group ($n = 4$) and AP group ($n = 4$), the expression of PRMT6 was determined by qPCR, western blot and immunohistochemistry of placental tissue sections. ImageJ software was used to quantitatively analyze the imprinting strength and the relative absorbance of immunohistochemistry
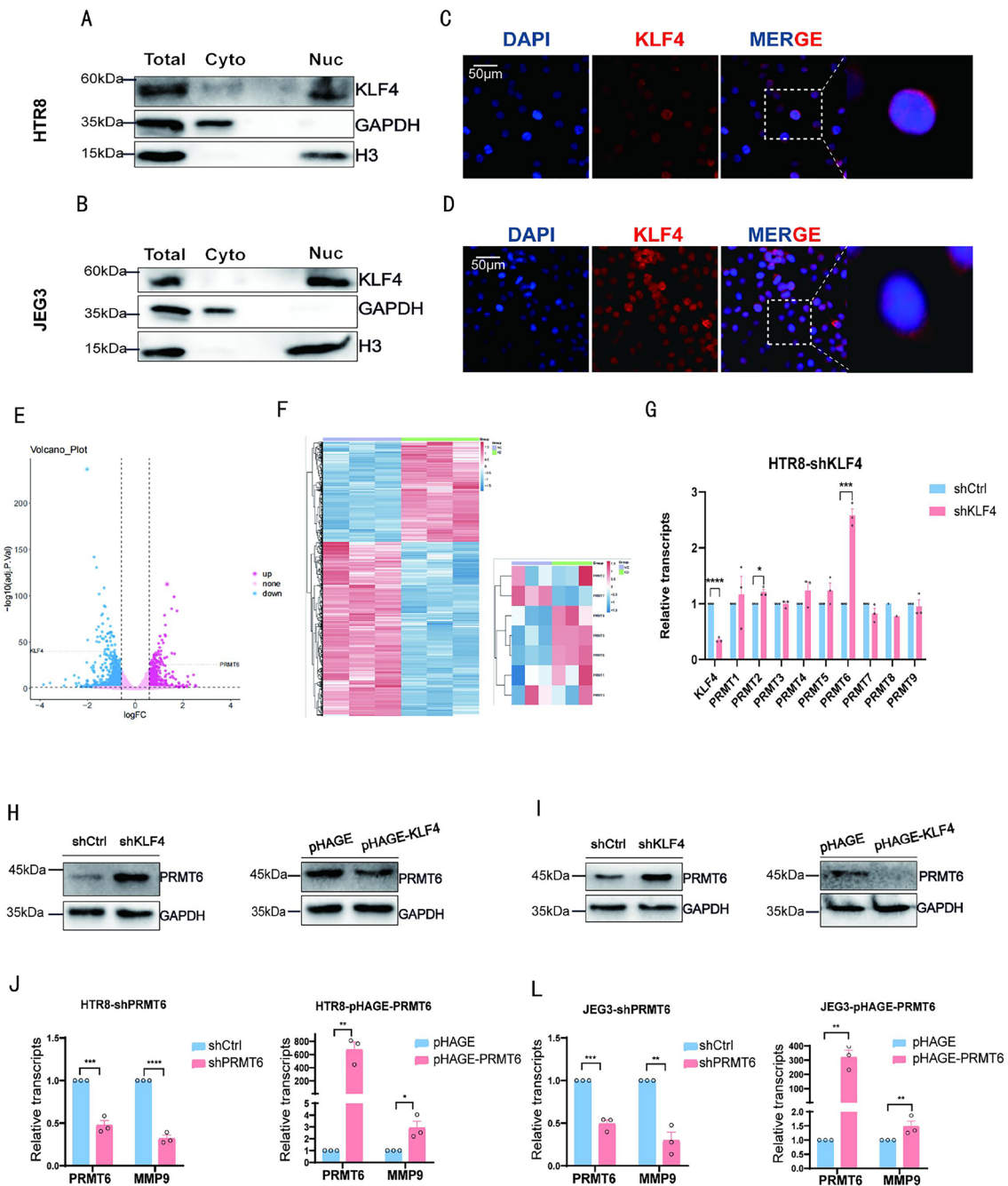
Tan *et al. Journal of Translational Medicine*   (2024) 22:922

Page 9 of 25

Fig. 3 (See legend on previous page.)

site to study the function of methylated modification of arginine by mutating arginine into alanine so that it can not be methylated, and western blot was used to detect changes in H3R2ME2a levels in the mutant (Fig. 4C–D), and the expression level of invasion and migration marker MMP9 (Fig. 4E–H) at the mRNA and protein levels. The results showed that MMP9 expression decreased in the H3R2 mutant trophoblast cell line. Wound healing

and transwell assays of the H3R2 mutant trophoblast cell line revealed that migration and invasion abilities were reduced (Fig. 4I, J). The expression of EMT-related proteins E-cadherin, N-cadherin, and vimentin was analyzed in trophoblast cells of H3R2 mutant by measuring mRNA and protein levels and observed that the expression of E-cadherin increased in the mutant cell line, while N-cadherin and vimentin expression decreased,
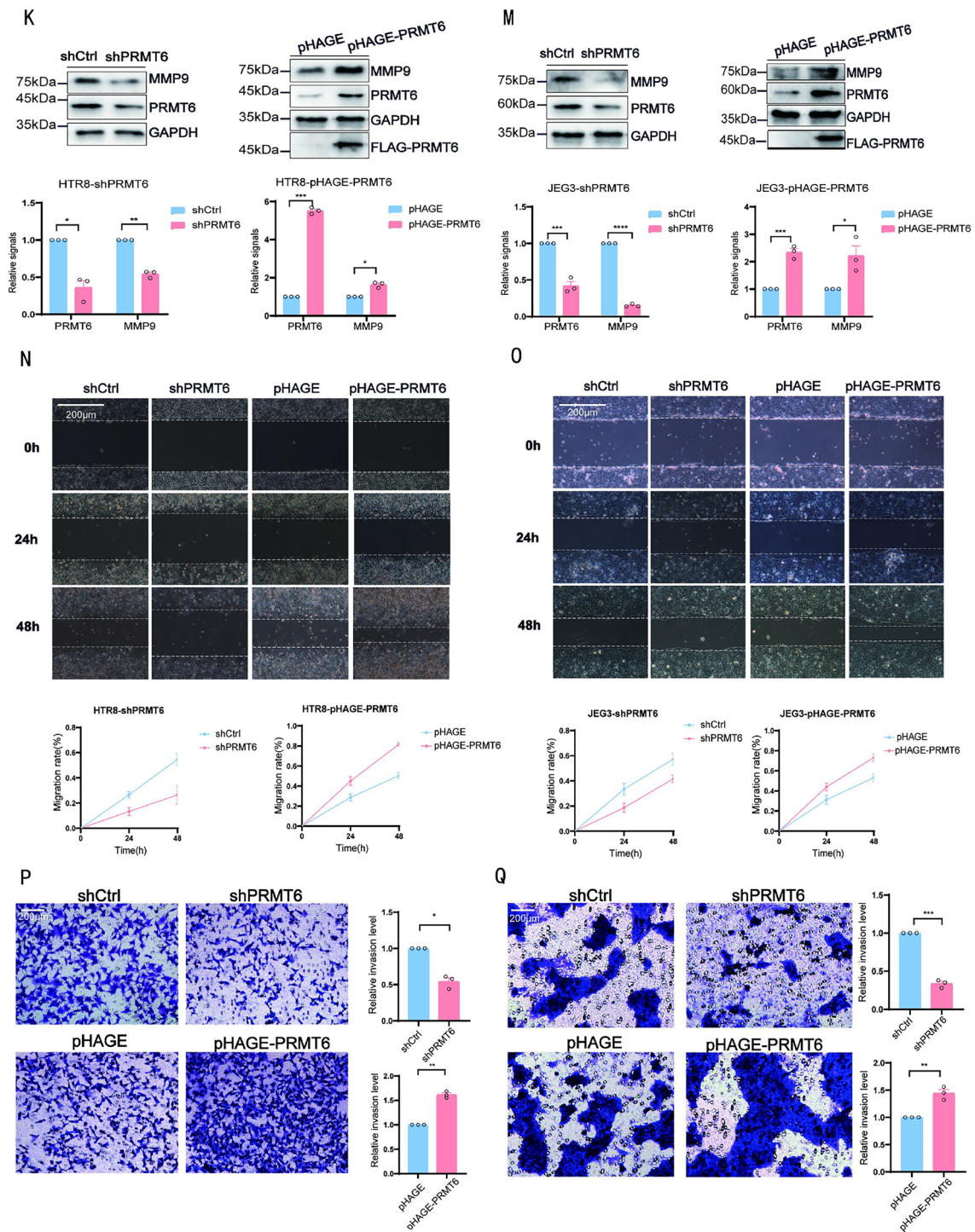
Tan *et al. Journal of Translational Medicine*　　(2024) 22:922

Page 10 of 25

Fig. 3 continued

indicating that the EMT of the H3R2 mutant trophoblast cell line was inhibited (Fig. 4M–P).

To determine the level of H3R2ME2a in the placental villi, H3R2ME2a expression in villi samples from normal pregnant women and URSA patients was determined using western blot and discovered that H3R2ME2a protein levels decreased in the villi tissue of URSA (Fig. 4Q). These results were confirmed
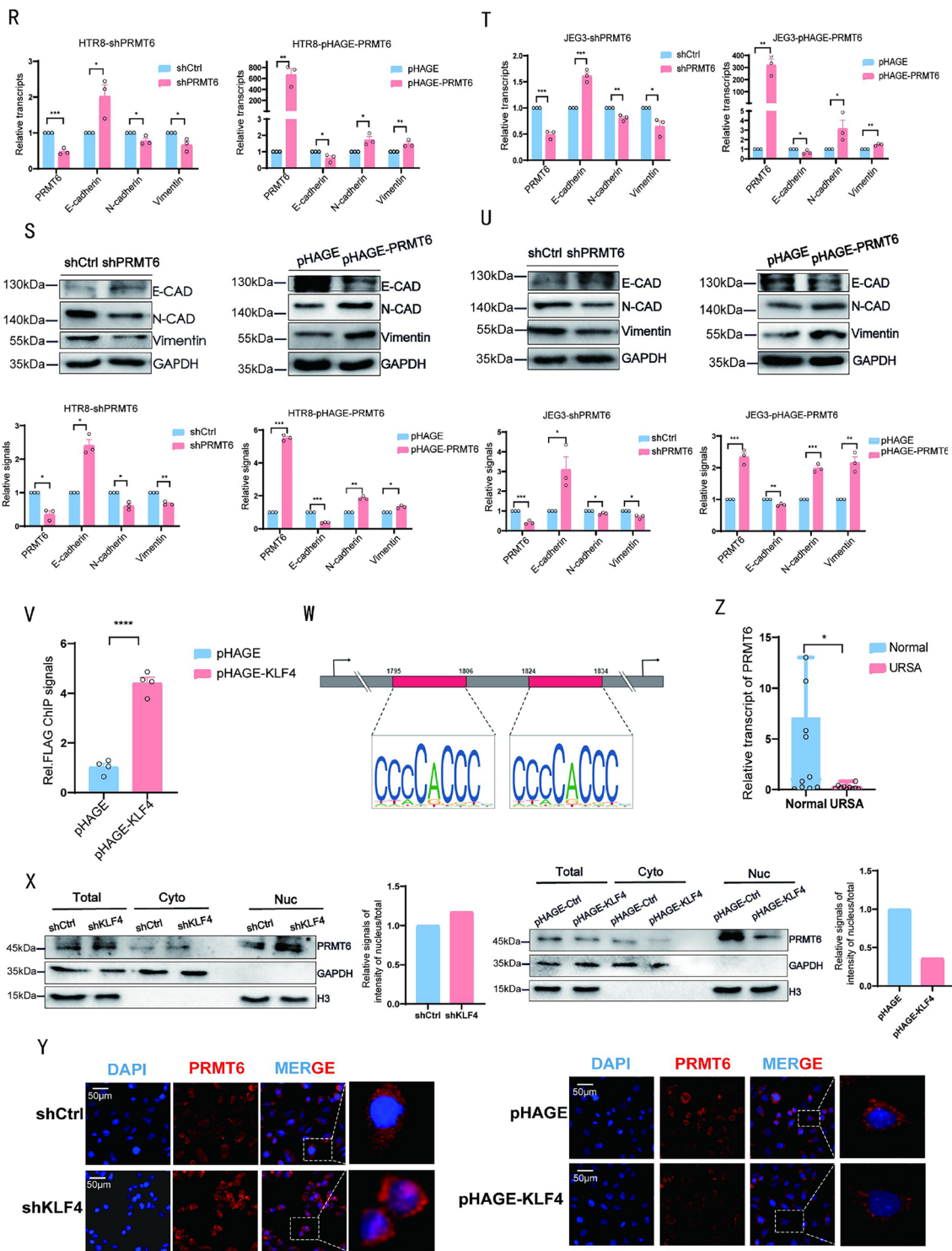
Fig. 3 continued

by immunohistochemical staining of villus tissue sections from URSA patients and normal pregnant women (Fig. 4R). Westernblot and IHC were used to detect

H3R2ME2a levels in the placental tissue of NP and AP mice, and it was found that H3R2ME2a expression decreased in the placental tissue of AP mice compared
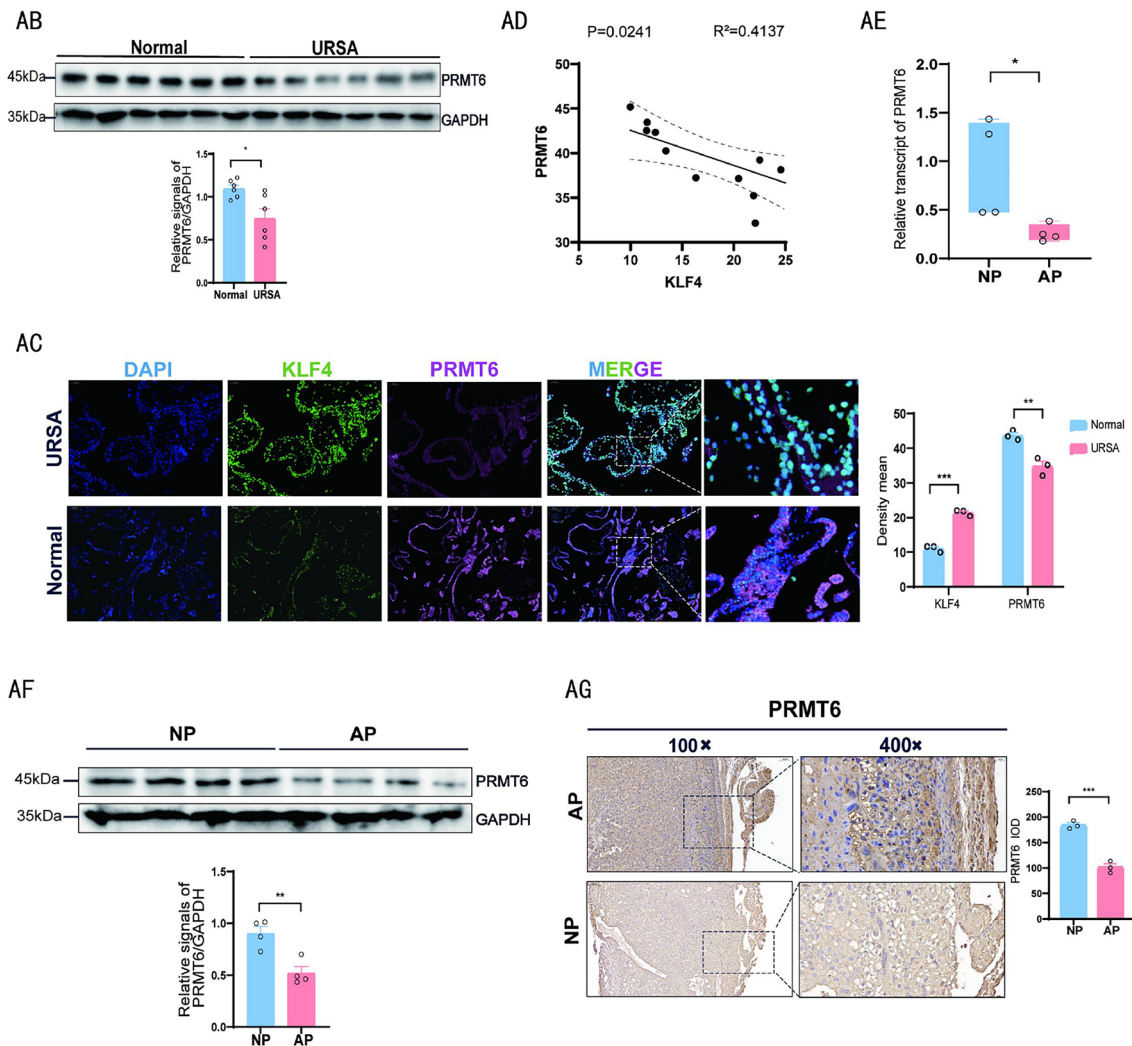
Fig. 4 PRMT6 inhibited the level of asymmetric methylation of arginine at histone H3R2 site. **A**, **B** The expression levels of H3R2ME2a in trophoblast cell lines with knockdown and overexpression of PRMT6 were determined respectively by western blot. **C**, **D** HTR8 and JEG3 cell lines mutated at H3R2 site were constructed, and the expression level of mutant H3R2ME2a was verified by western blot.The protein imprinting strength was quantitatively analyzed by ImageJ software. **E**–**H** The levels of invasion and migration marker MMP9 in mutant trophoblast cell line at H3R2 site were determined by qPCR and western blot. The protein imprinting strength was quantitatively analyzed by ImageJ software. **I**, **J** Wound healing scratches were imaged immediately, 24 h and 48 h after initial scratch time to quantify relative migration, quantifying relative migration using ImageJ software. **K**, **L** HTR8 cells and JEG3 cells were suspended in serum-free medium and then inoculated into an insertion chamber pre-coated with diluted matrix gel and incubated for 48 h for invasion determination. Cells at the lower surface of the membrane were counted and analyzed under a light microscope in three random fields of view. The staining intensity was quantified using the ImageJ software. **M**–**P** The expression levels of E-cadherin, N-cadherin and vimentin markers of epithelial mesenchymal transformation in mutant trophoblast cell line at H3R2 site were determined by qPCR and western blot. The imprinting strength of proteins was quantitatively analyzed by ImageJ software. **Q** The expression of H3R2ME2a protein in chorionic villus of normal pregnancy patients ($n=7$) and URSA patients ($n=7$) was determined by western blot. The protein imprinting strength was quantified using ImageJ software. **R** The expressions of H3R2ME2a protein in villi of normal pregnancy patients ($n=3$) and URSA patients ($n=3$) were determined by immunohistochemical. The staining intensity was quantified by ImageJ software. **S-T** In NP group ($n=4$) and AP group ($n=4$), the expression of H3R2ME2a was determined by western blot and immunohistochemistry of placental tissue sections. ImageJ software was used to quantitatively analyze the imprinting strength and the relative absorbance of immunohistochemistry
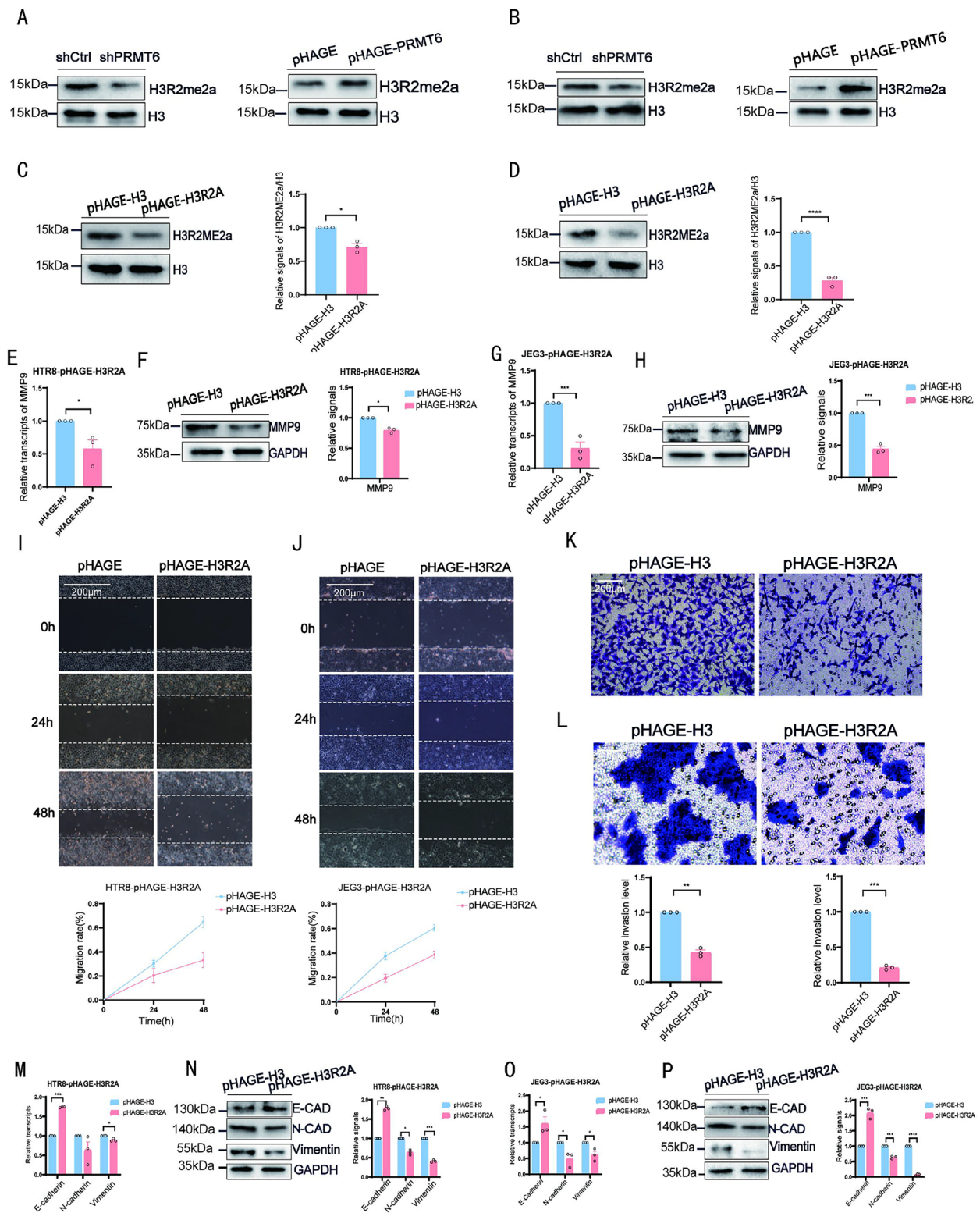
Fig. 4 (See legend on previous page.)

Tan *et al. Journal of Translational Medicine*   (2024) 22:922
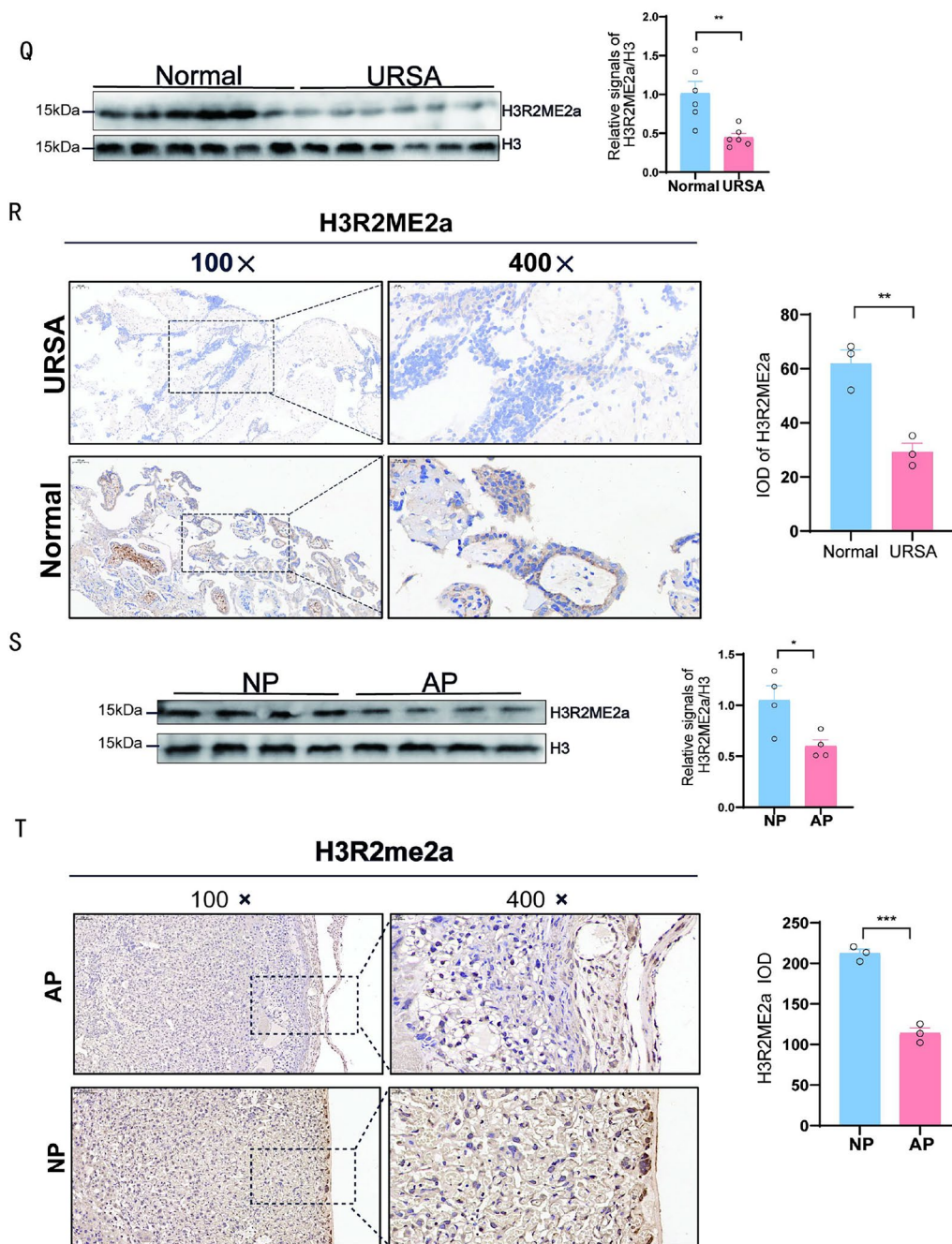
Page 14 of 25

Fig. 4 continued

to that in NP mice (Fig. 4S, T). These data indicated that H3R2ME2a levels were significantly downregulated in the URSA female villi and placental tissues of aborted mice. PRMT6 can mediate the pathological process of URSA through H3R2ME2a, although the specific mechanism has not been elucidated.

KLF4 regulates the level of H3R2ME2a by regulating PRMT6 and then regulates the biological behaviors of trophoblast cells, such as invasion, migration, and EMT

Our results demonstrated that KLF4 regulates PRMT6 expression and PRMT6 regulates the asymmetric methylation of arginine at the histone H3R2 site; however, the relationship between KLF4, PRMT6, and H3R2ME2a remains unknown. We discovered that

PRMT6 overexpression in KLF4 overexpressing HTR8 cells reversed the expression of H3R2ME2a (Fig. 5A). Contrarily, PRMT6 knockdown in KLF4 knockdown HTR8 cells decreased the expression of H3R2ME2a (Fig. 5B). These results indicate that KLF4 can regulate the expression of H3R2ME2a via PRMT6. ChIP analysis showed that KLF4 deletion significantly increased the enrichment of H3R2ME2a at MMP9, N-cadherin, and vimentin promoter sites and decreased the enrichment of E-cadherin promoter sites (Fig. 5C). These results indicated that the KLF4-PRMT6-H3R2ME2a axis regulates the transcription of genes related to trophoblast cell invasion, migration, and EMT. At the mutant H3R2 site in KLF4 knockdown HTR8 cell line, the increased level of invasion-related gene MMP9 protein was inhibited, as well as the expression of EMT-related genes N-cadherin and vimentin protein, and the decreased level of E-cadherin protein was inhibited (Fig. 5D). Wound healing and transwell assays of trophoblast cell lines with KLF4 knockdown and H3R2 mutation revealed that the increased migration and invasion abilities of trophoblast cell lines by KLF4 knockdown were inhibited (Fig. 5E–H). These results indicated that KLF4 regulates the invasion, migration, and EMT of trophoblast cells through H3R2ME2a, and mutation at the H3R2 site can inhibit the changes in trophoblast cell invasion, migration, and EMT induced by KLF4. Moreover, in PRMT6 overexpressing HTR8 cell line with a mutated H3R2 site, the increase of invasion-related gene MMP9 protein level was inhibited, as well as EMT-related gene N-cadherin and vimentin protein expression, while the reduction of E-cadherin protein was inhibited (Fig. 5I). Wound healing and transwell assays of PRMT6 overexpressing trophoblast cell lines with mutated H3R2 revealed that the increased migration and invasion abilities in overexpressed PRMT6 trophoblast cell lines were inhibited (Fig. 5J–M). These results indicated that PRMT6 regulates the invasion, migration, and EMT of trophoblast cells through H3R2ME2a, and mutation in the H3R2 site can inhibit PRMT6-induced changes in the invasion, migration, and EMT of trophoblast cells.

In summary, KLF4 can inhibit the asymmetric methylation of arginine residues at the H3R2 site by inhibiting PRMT6 transcription and nucleation. Moreover, the KLF4-PRMT6-H3R2Me2a axis can regulate the transcription of genes related to trophoblast cell invasion, migration, and EMT. Regulation of trophoblast cell invasion, migration, EMT, and other biological behaviors may change the biological behavior and function of villi tissue.

Inhibition of KLF4 can inhibit embryo absorption in miscarried mice

We first conducted in vivo studies using models of normal pregnancy and aborted mice to determine whether KLF4 affects pregnancy outcomes. KLF4 expression was increased at the placental interface of aborted mice compared to NP mice (Fig. 1K–N). We activated KLF4 by intraperitoneal injection of KLF4 agonist APTO-253 on days 6.5, 8.5, 10.5, and 12.5 in NP mice, and discovered that the embryonic absorption rate increased compared to the control group (Fig. 6A). Protein immune imprinting revealed that the expression levels of PRMT6 and H3R2ME2a were decreased in mouse placenta (Fig. 6B). IHC confirmed that the expression levels of N-cadherin and vimentin were decreased, while the expression levels of E-cadherin were increased after the injection of APTO-253 (Fig. 6C). KLF4 was inhibited by intraperitoneal injection of

(See figure on next page.)

Fig. 5 KLF4 regulates the level of H3R2ME2a by regulating PRMT6, and then regulates the biological behaviors of trophoblast cells such as invasion, migration and EMT **A** The protein level of H3R2ME2a in the control group, the over-expressing KLF4 group, the over-expressing PRMT6 group, and both overexpressing KLF4 and PRMT6 group detected by western blot. **B** The protein level of H3R2ME2a in the control group, the knockdown KLF4 group, the knockdown PRMT6 group, and both knockdown KLF4 and PRMT6 group detected by western blot. **C** The H3R2ME2a concentrations of MMP9, E-cadherin, N-cadherin and vimentin promoters in HTR8 with KLF4 knockdown were analyzed by ChIP-qPCR. **D** The protein level of H3R2ME2a and invasion and migration related proteins MMP9 and EMT-related proteins E-cadherin, N-cadherin and vimentin in control group, knockdown KLF4 group, H3R2 site mutant, and simultaneously knockdown KLF4 group and mutation H3R2 site HTR8 cell line by western blot. **E**, **F** Wound healing scratches were imaged immediately, 24 h and 48 h after initial scratch time to quantify relative migration, quantifying relative migration using ImageJ software. **G**, **H** HTR8 cells and JEG3 cells were suspended in serum-free medium and then inoculated into an insertion chamber pre-coated with diluted matrix gel and incubated for 48 h for invasion determination. Cells at the lower surface of the membrane were counted and analyzed under a light microscope in three random fields of view. The staining intensity was quantified using the ImageJ software. **I** The protein level of H3R2ME2a and invasion and migration related proteins MMP9 and EMT-related proteins E-cadherin, N-cadherin and vimentin in control group, over-expressing PRMT6 group, H3R2 site mutant, and simultaneously over-expressing PRMT6 group and mutation H3R2 site HTR8 cell line by western blot. **J**, **K** Wound healing scratches were imaged immediately, 24 h and 48 h after initial scratch time to quantify relative migration, quantifying relative migration using ImageJ software. **L**, **M** HTR8 cells and JEG3 cells were suspended in serum-free medium and then inoculated into an insertion chamber pre-coated with diluted matrix gel and incubated for 48 h for invasion determination. Cells at the lower surface of the membrane were counted and analyzed under a light microscope in three random fields of view. The staining intensity was quantified using the ImageJ software
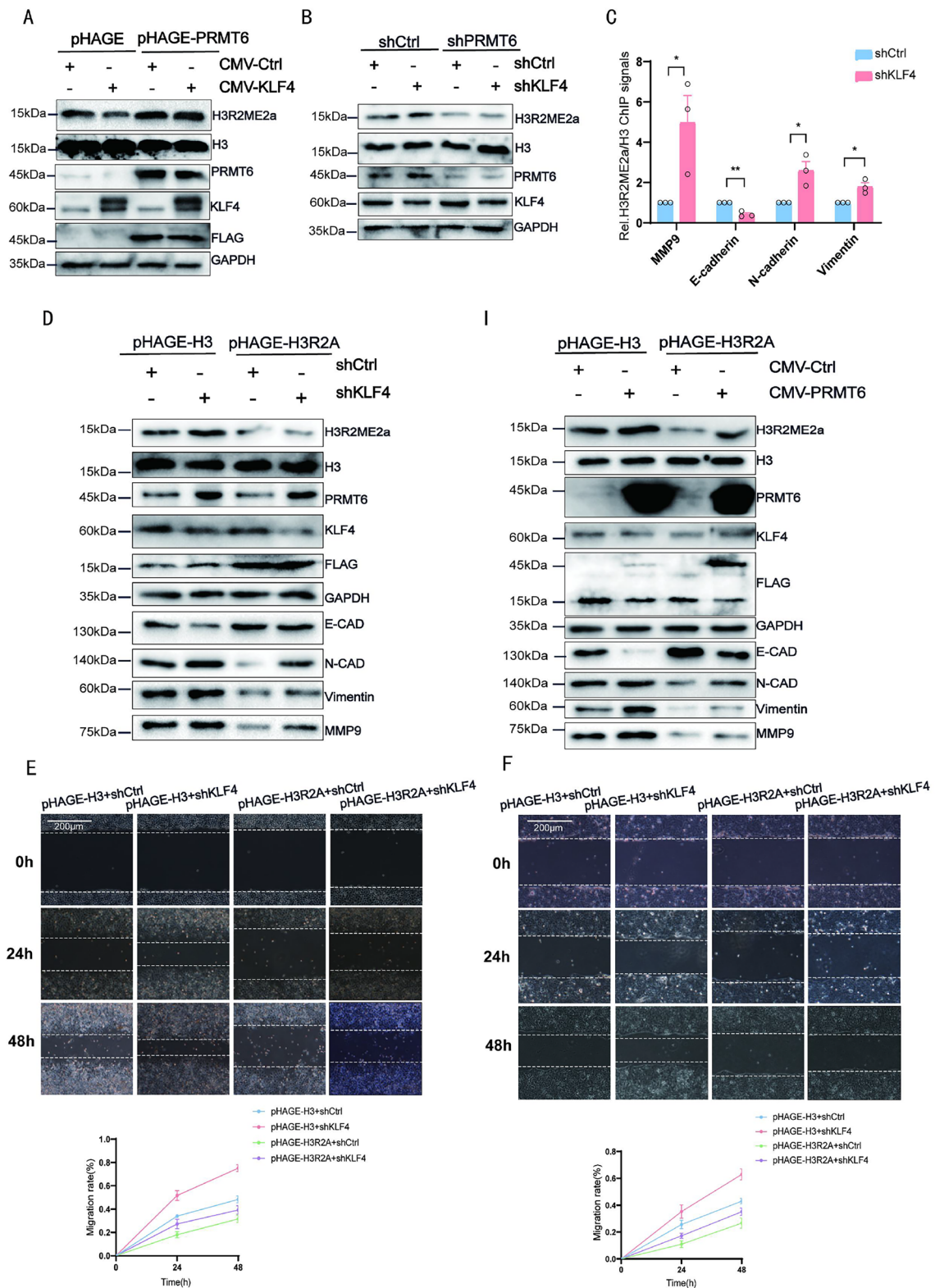
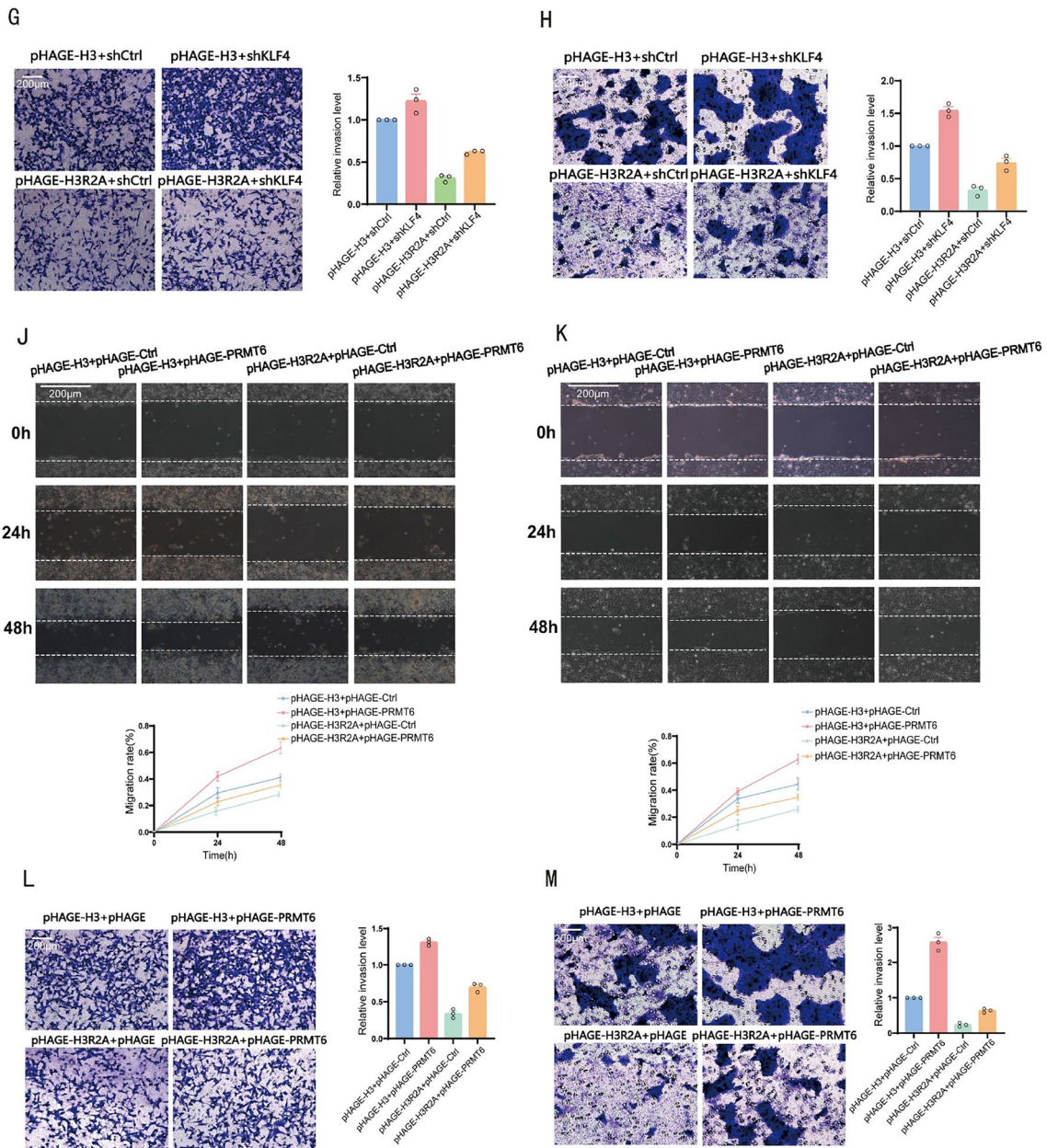**Fig. 5** (See legend on previous page.)

Fig. 5 continued

Fig. 6 Inhibition of KLF4 can inhibit embryo absorption in miscarried mice. **A** Representative macroscopic views of the uterus in NP mice with and without APTO-253 injected treatment. **B**–**C** The expression of PRMT6 and H3R2ME2a protein in placental tissue sections was determined by western blot. The expression of E-cadherin, N-cadherin, vimentin was determined by immunohistochemical. **D** Representative macroscopic views of the uterus in NP and AP mice, with and without Kenpaullone injected treatment, with and without EPZ020411 gavaged treatment. **E**–**F** The expression of H3R2ME2a protein in placental tissue sections was determined by western blot. The expression of E-cadherin, N-cadherin, vimentin was determined by immunohistochemical. The protein imprinting strength and the staining intensity was quantified using ImageJ software.The protein imprinting strength and the staining intensity was quantified using ImageJ software
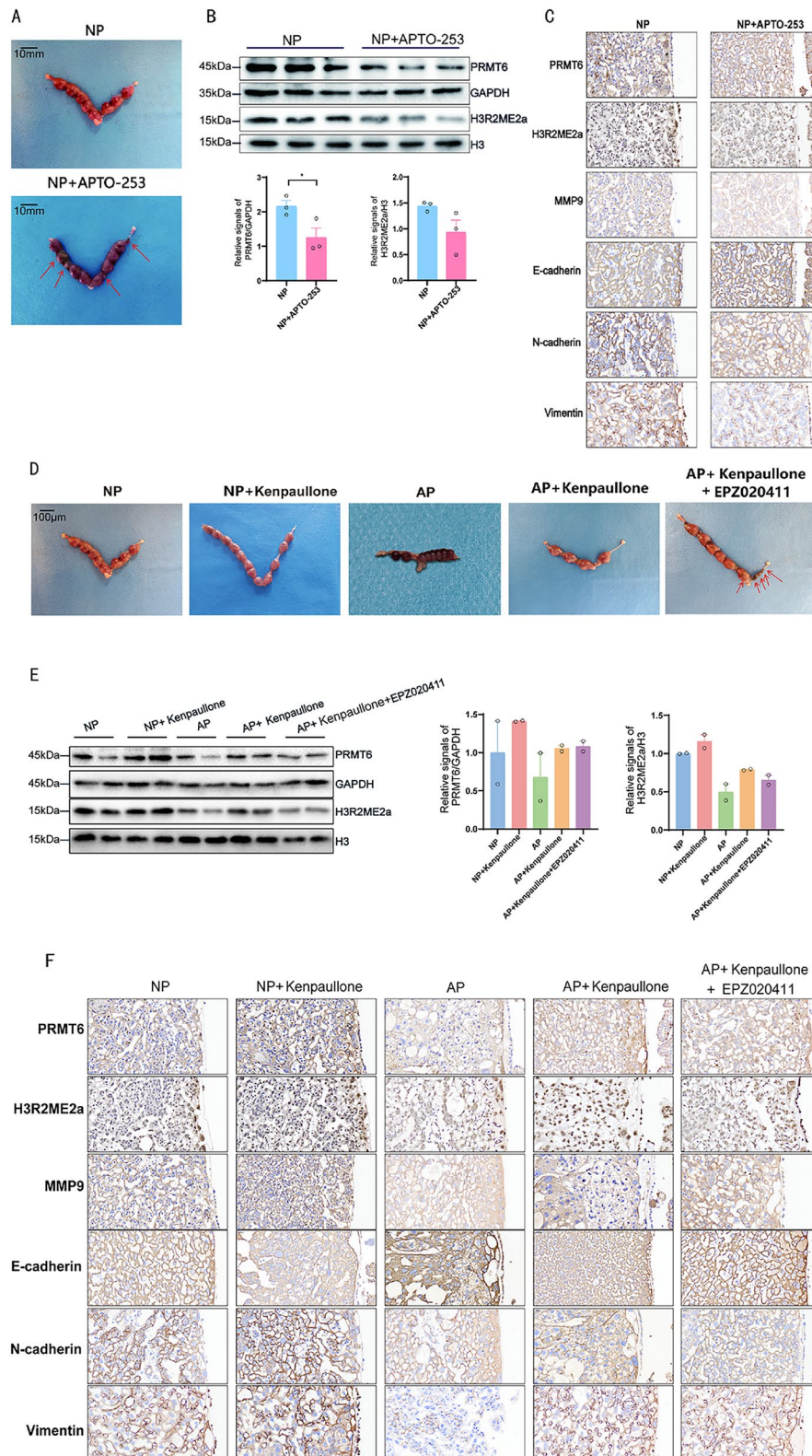
Tan *et al. Journal of Translational Medicine*   (2024) 22:922

Page 18 of 25

Fig. 6 (See legend on previous page.)

Tan *et al. Journal of Translational Medicine*   (2024) 22:922

Page 19 of 25

KLF4 inhibitor kenpaullone on days 6.5, 8.5, 10.5, and 12.5. The embryo absorption rate was assessed on day 13.5 of gestation. The results revealed that the embryo absorption rate of mice in the AP group was higher than that of the mice in the NP group. The embryo absorption rate of mice treated with kenpaullone was decreased, while the embryo absorption rate was higher in mice injected with kenpaullone and PRMT6 inhibitor EPZ020411 (Fig. 6D). Moreover, western blot revealed that H3R2ME2a expression decreased in the placental tissue of mice in the AP group, whereas kenpaullone treatment increased this expression, which could be reversed by EPZ020411 administration. KLF4 regulates H3R2ME2a expression via PRMT6 (Fig. 6E). This was confirmed by the IHC results, which showed that E-cadherin expression in the placenta of mice in the AP group was significantly higher than that of mice in the NP group, while the expression of N-cadherin and vimentin was significantly lower than that of mice in the NP group. Kenpaullone treatment reversed the upregulation of E-cadherin and downregulation of N-cadherin and vimentin in the placenta of mice in the AP group. However, this phenomenon was suppressed in mice simultaneously administered Kenpaullone and EPZ020411 via gavage (Fig. 6F). Our study confirmed that KLF4 inhibition mitigated fetal abortion in aborted mice by promoting the expression of PRMT6, H3R2ME2a, and EMT in trophoblast cells.

Discussion

Chromosomal structural abnormalities, anatomical abnormalities, infections, endocrine abnormalities, and immune dysfunction, as well as environmental factors, including smoking and alcohol use, influence the development of RSA [21]. However, the pathogenesis of URSA remains unknown. KLF4 is a zinc-finger-type transcription factor that negatively regulates EMT in various gastrointestinal cancers through crosstalk with the TGF-β, Notch, and Wnt signaling pathways [22]. Besides, KLF4 can function as a stress response gene induced by various harmful stimuli to support cell survival [23]. In this study, by analyzing the transcriptome of the villus tissue of URSA patients in the database and clinical samples, we discovered that abnormally elevated KLF4 expression may induce URSA. An abnormal increase in KLF4 was also observed in the placental tissue of mice with spontaneous abortion induced by intraperitoneal injection of LPS; intraperitoneal injection of a KLF4 inhibitor could effectively improve the abortion outcome. Intraperitoneal injection of KLF4 agonist increased embryo absorption in NP mice. Therefore, elevated KLF4 expression may be one of the most critical factors leading to URSA.

Placental trophoblast cells can regulate their biological behavior through epigenetic reprogramming, thereby affecting the pregnancy outcome. In this study, the transcriptome data of KLF4 knockdown cells were analyzed, and it was revealed that KLF4 negatively regulated the transcription level of PRMT6. What's more, KLF4 can inhibit PRMT6 nuclear translocation. Although we haven't investigated the exact mechanism, we think KLF4 may affect the nuclear translocation of PRMT6 in the following ways. Fist, KLF4 may promote PRMT6 to interact with specific proteins: PRMT6 enzymes may be guided into the nucleus through interactions with other proteins. For example, in the study of host cell iron death induced by PtpA in Mycobacterium tuberculosis, PtpA interacts with host arginine methyltransferase PRMT6 through its amino acid domain at position 1–50 and promotes trimethylation of arginine at position 2 of H3 histone (H3R2ME2a). This suggests that PRMT6 may be guided into the nucleus through interactions with specific proteins [24]. Second, KLF4 can regulate the expression of proteins related to cell localization: KLF4 can regulate the expression of proteins related to cell localization and thus regulate the subcellular localization of downstream target genes. One of the KLF family homologue erythroid Krüppel-like Factor (EKLF/KLF-1), can bind two nuclear localization signals importin α and importin β target EKLF to the nucleus which suggests that transport relies primarily on a novel zinc finger/importin protein interaction [25]. In mouse embryonic stem (ES) cells, KLF2 and KLF4 function redundantly to drive high level expression of KPNA2, which can code Importin-α1, a localization signal belongs to a receptor family that recognizes classical nuclear [26]. These researches suggest that KLF4 may regulate the nuclear localization of downstream target genes by influencing the expression of cell localization proteins.Nxt but not least, PRMT6 needs to enter into nucleus to perform its function: KLF4 regulates the level of the level of asymmetric methylation of arginine at the histone H3R2 site by regulating PRMT6 and then regulates the biological behaviors of trophoblast cells. Histone H3 is localized in the nucleus and PRMT6 may therefore need to enter the nucleus to exert its methyltransferase activity on histone H3, thereby altering the expression of H3R2ME2a. PRMT6 may be guided into the nucleus by participating in these modification processes. Trophoblast cell methylation may be significantly correlated with various biological behaviors, including invasion and migration. N6-methyladenosine (m6A), the most common and extensively studied type of RNA modification in eukaryotic mRNAs, is regulated by m6A methyltransferase and demethylase. In the regulation mechanism of m6A methylation, methyltransferase 14 (METTL14) can increase the expression of FOXO3a through m6A

Tan *et al. Journal of Translational Medicine*   (2024) 22:922

Page 20 of 25

dependent mechanism, inducing autophagy and trophoblast apoptosis and inhibiting trophoblast proliferation and invasion [27]. Demethylase ALKBH5 can regulate the stability of CYR61 mRNA through m6A modification to inhibit trophoblast invasion [28]. In human villi explants, ALKBH5 knockdown promoted trophoblast invasion in vitro, while ALKBH5 overexpression inhibited these effects [29, 30]. After ALKBH5 overexpression, E-cadherin expression was upregulated, and N-cadherin, vimentin, MMP2, and MMP9 expression was downregulated. In vivo studies have shown a significant increase in fetal abortion rates and a significant decrease in fetal and placental weight in mice with trophoblast ALKBH5-specific knockout [31]. Studies have revealed that the 36-position lysine trimethylation modification (H3K36me3) on histone H3 can be recognized by METTL14, thus dynamically and specifically mediating the occurrence of m6A methylation during transcription, which raises the question of whether histone modification may affect the biological behavior of trophoblasts [32]. Recent research has revealed that some histone methylation modifications in trophoblast cells can regulate their biological behavior, and abnormal levels of histone methylation modifications may lead to pathological changes. For example, H3K9/27ME3 is associated with differential expression of matrix metalloproteinases in the placenta, which can regulate the dynamic process of placental implantation in the mother, and its abnormal expression may lead to eclampsia [33]. However, the effects of histone methylation modification on the biological behavior and specific regulatory mechanisms of trophoblast cells remain poorly understood. H3R2ME2a is asymmetric methylation at histone H3R2 mediated by PRMT6, which can mediate inflammation and apoptosis in human umbilical vein endothelial cells [34]. The invasion and migration of osteosarcoma cells U2OS can also be inhibited by blocking Thrombospondin-1 (TSP-1), a negative regulator of angiogenesis and cell migration [35]. Our results revealed that, by binding to the PRMT6 promoter, KLF4 can inhibit its transcription and entry into the nucleus to reduce the methylation level of arginine residues at the histone H3R2 site. A histone H3R2 mutant trophoblast cell line was created to determine changes in cell biological behavior after reduced arginine methylation at the H3R2 site. The results revealed that invasion, migration, and EMT of the H3R2 mutant trophoblast cell line were inhibited. ChIP analysis demonstrated that KLF4 knockdown increased the enrichment of H3R2ME2a in the MMP9, N-cadherin, and vimentin promoter regions and decreased the enrichment of H3R2Me2a in the E-cadherin promoter region. These results indicate that KLF4 regulates the invasion, migration, and EMT behaviors of trophoblast cells through

H3R2ME2a. In H3R2 mutant cell lines, KLF4 knockdown or PRMT6 overexpression could not fully compensate for trophoblast cell invasion, migration, and epithelial-mesenchymal capacity, confirming this conclusion. The levels of H3R2ME2a decreased in placental tissues of mice with an abortive tendency induced by intraperitoneal injection of LPS and recovered after treatment with KLF4 inhibitor, which could be inhibited by gavage of PRMT6 inhibitor. These results demonstrate a potential mechanism for adverse pregnancy outcomes caused by abnormally elevated KLF4 expression in placental tissues and may also consider the potential clinical significance of KLF4 inhibitors in the treatment of patients with URSA.

This study has several limitations. First, KLF4 may have multiple regulatory mechanisms to control cell biological behavior, and whether pregnancy outcome can be ultimately regulated through other mechanisms needs further investigation. Second, PRMT6 may have multiple methylation sites that regulate the biological behavior of trophoblast cells. In this study, we focused only on the histone H3R2 site and ignored other possible methylation sites. Next, in our study, although HTR8 and JEG3 were utilized as cell models, there was a lack of primary trophoblast cells to investigate cellular functions and molecular mechanisms while the primary trophoblasts may be more consistent with human characteristics and present more reliable results, which needs to be improved in subsequent studies. Finally, the results of this study in mice were obtained through injection of inhibitors and agonists, which may have other non-specific targets of action and unknown effects on the pregnancy outcome. These limitations indicate that the findings of this study should be interpreted with caution.

Conclusions
This study provides new insights into the unique biological behaviors regulated by KLF4 of trophoblast cells in early pregnancy. Our results indicate that KLF4 inhibits the expression level of H3R2ME2a in trophoblast cells by regulating the transcriptional level and nuclear translocation of PRMT6. Especially, the enrichment of H3R2ME2a at N-cadherin and vimentin and MMP9 promoter sites was downregulated by KLF4 while E-cadherin was upregulated. The KLF4-PRMT6-H3R2ME2a axis regulates trophoblast cell invasion, migration, and EMT, thereby plays important role in maintaining successful pregnancy (Fig. 7). These findings inform the possible pathogenesis of URSA as well as potential therapeutic options.

Materials and methods
Patients and tissue samples
This study included 15 patients who terminated their pregnancies for non-medical reasons (normal pregnancy,

Tan *et al. Journal of Translational Medicine*   (2024) 22:922
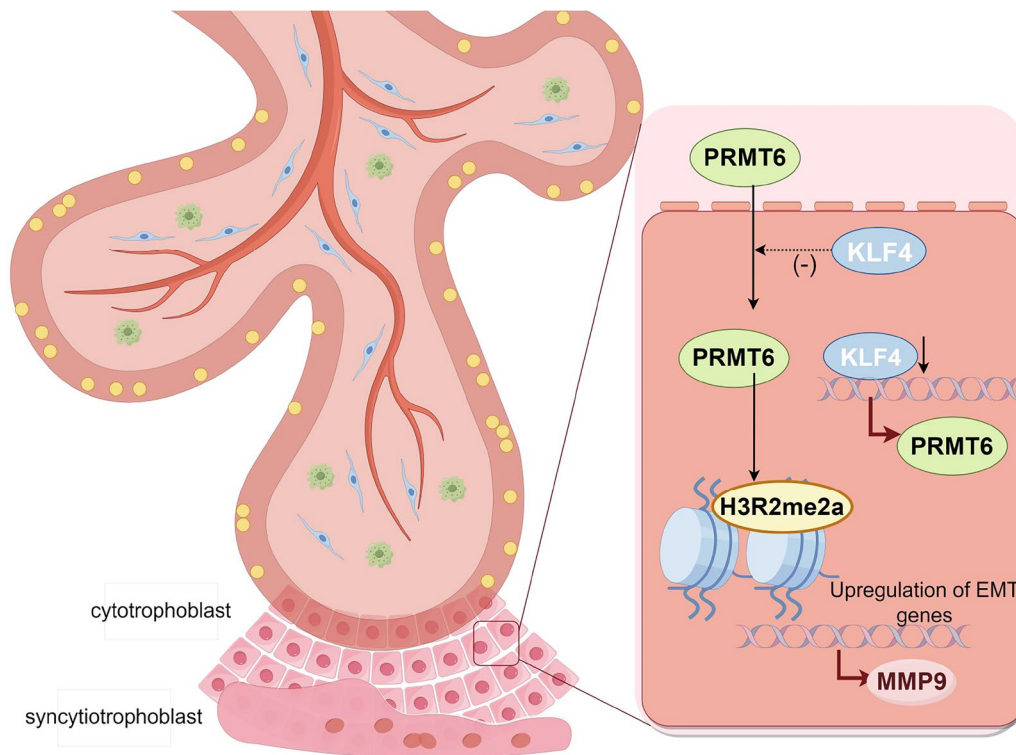
Page 21 of 25

Fig. 7 The KLF4/PRMT6/H3R2ME2a axis regulates mechanisms associated with unexplained recurrent spontaneous abortion by regulating trophoblast function

NP group) and 12 patients with URSA two or more times (URSA group). The study enrolled patients treated in Renmin Hospital of Wuhan University from October,2021 to January,2023. Patients in the NP group had a history of more than one live birth, with no history of adverse pregnancy, including spontaneous abortion, eclampsia, and preterm birth. URSA patients with the following characteristics were excluded: [1] abnormal anatomical structure of the reproductive tract [2], chromosomal abnormalities in parents or embryos [3], infectious diseases, and [4] endocrine or metabolic diseases. These patients had an abortion between seven and nine weeks of gestation to terminate the unintended pregnancy. Baseline data from the recruited patients are listed in Table S1. After complete curettage of uterine cavities, samples were collected immediately and washed with Phosphate-buffered saline (PBS). The villous tissue was completely separated, partially fixed in 4% paraformaldehyde, embedded in paraffin wax, partially frozen, and stored in liquid nitrogen. All procedures were approved by the Ethics Committee of Renmin Hospital of Wuhan University (No. WDRY2021-K044). Patients with a normal pregnancy and URSA who underwent an induced abortion provided written informed consent. The

procedures used in this study adhere to the tenets of the Declaration of Helsinki.

Animals and experimental protocol

The 8-week-old female C57BL/6 mice and 8-week-old male BALB/C mice were kept in a specific pathogen-free (SPF) environment under standard environmental conditions (22–24 °C and 60–70% relative humidity). After adaptive feeding, female mice mated with male mice in a 2:1 ratio. The day the embolus was visible was recorded as day 0.5 of the embryo (E0.5). The mice were divided into five groups (three mice per group). Abortion was induced by injecting lipopolysaccharide (LPS) solution (0.25 mg/kg; Sigma) intraperitoneally at E7.5. The control group was injected with normal saline. The control+KLF4 agonist APTO-253 group was intraperitoneally injected every other day for one week (MCE, Shanghai; 1 μg/g) with normal saline as described above. The control+KLF4 inhibitor kenpaullone and abortion+kenpaullone groups were intraperitoneally injected for one week on alternate days (MCE, Shanghai; 1 μg/g) with LPS and normal saline, respectively, as described above. The abortion+kenpaullone+PRMT6 inhibitor EPZ020411 group was intraperitoneally injected every other day for one week (MCE, Shanghai; 1 μg/g),

Tan *et al. Journal of Translational Medicine* (2024) 22:922

Page 22 of 25

continuous intragastric administration of EPZ020411 (MCE, Shanghai; 10 mg/kg) for one week and LPS injections as described above. Mice were killed with isoflurane at E13.5, and the uteroplacental complex was collected for further analysis. The embryo absorption rate of each mouse was determined to evaluate the pregnancy outcome, defined as the number of reabsorbed embryos/(number of reabsorbed embryos + number of viable fetuses) × 100%. All protocols and experiments were approved by the Animal Care and Use Committee of Wuhan University (approval number: 20190710).

Cell culture, treatment, and transfection

Human trophoblast cell line HTR8/SVneo (HTR8) was cultured in RPMI 1640 medium (Gibco, USA), and JEG-3 cells were cultured in Minimum Essential Medium Eagle (MEM) (HyClone, USA). HEK-293T cells were cultured in Dulbecco's modified Eagle's medium (DMEM) (Gibco, USA) with 10% fetal bovine serum (FBS) (Gibco, USA) and 1% antibiotic and incubated at 37 °C in the presence of 5% CO_2.

KLF4 shRNA, control shRNA, KLF4 overexpression plasmid, and empty vector plasmid were purchased from Paivi Biosciences Inc. Expression plasmids for PRMT6, H3, and knockdown for PRMT6 were constructed using standard molecular biology techniques. Point mutations were created by site-directed mutagenesis.

HEK-293T cells were cultured to 70–80% confluence and then transfected with 2 μg target plasmids, 1 μg psPAX2, and 1 μg pMD2.G plasmids using the Neofect reagent(TF20121201, Neofect (Beijing) bioyech Co.ltd). After 48 h, the supernatant-containing lentivirus was collected and filtered through a 0.22 μm filter. HTR8 and JEG3 cells were infected with lentivirus with 8 μg/mL polybrene. After 24 h, HTR8 and JEG3 cells were selected using 2.5 μg/mL puromycin.

Collection data set

From the GEO database (https://www.ncbi.nlm.nih.gov/geo/) for recurrent miscarriage, GSE121950-related data [17] containing three reference samples and three samples of recurrent miscarriage were collected. The limma package was used to standardize and normalize the data.

Analysis of data

(1) Difference analysis.
(2) First, the limma package was used for differential expression analysis of the data. The screening conditions were set as |log2FC|> 1 and $P < 0.05$. The volcano map was drawn using ggVolcano. The top 100 genes were displayed on heatmap using pheatmap.

(3) Functional enrichment analysis.
(4) Enrichment analysis of the differentially expressed genes was performed. The clusterProfiler package was used for GO enrichment analysis, and the screening condition was $P < 0.05$. The top 10 GO biological processes were shown on a bubble map drawn using the ggplot2 package. KEGG enrichment analysis was performed using clusterProfiler packages, and the screening condition was $p < 0.05$. The GOplot package was used for visualization.
(5) Protein-protein interaction network and submodule analysis.
(6) The STRING website was used to screen the core genes for protein interaction analysis, with an interaction score threshold of 0.4 (medium correlation). The interaction network was visualized using Cytoscape software (version 3.9.1). To further screen core submodules, topological algorithm analysis, including DMNC, MNC, and EPC, was performed using Cytohubba software. The top 10 genes obtained by the three algorithms were intersected using the Venn diagram, and the last seven core genes were screened out.

RNA sequencing (RNA-seq)

Total RNA was extracted from HTR8 cells using TRIzol reagent RNAiso Plus (Takara). Library construction, sequencing, and bioinformatic analysis were performed by Wuhan Yingzi Gene Technology Co. Ltd.

Wound-healing assay

When the cells reached 80–90% confluence, the center of the plate was scratched using a 1 mL pipette, and the medium was replaced with one containing 1% FBS. The width of the scratch was recorded by photography at 0, 24, and 48 h. PBS was used to remove floating debris before each measurement.

Transwell invasion assay

The upper chamber of the Transwell insert was precoated with Matrix Matrigel (BD Biosciences, CA, USA) (1:9) for 4–12 h before the experiment. The Transwell insert was seeded with 5×10^4 cells in 200 μL serum-free medium, while 600 μL medium containing 10% FBS was filled in the lower chamber. HTR8 cells were added into the upper chamber with 8 μm pores, while JEG3 cells were added into the upper chamber with 12 μm pores and incubated at 37 °C for 48 h. The cells attached to the outside of the insert were fixed with 4% paraformaldehyde for 30 min and stained with crystal violet (Servicebio, China). Three random pictures were taken under the microscope to count the number of invaded cells.

Tan *et al. Journal of Translational Medicine*   (2024) 22:922

Page 23 of 25

Quantitative PCR analysis (RT-qPCR)

RNA was extracted from cells using TRIzol reagent RNAiso Plus (Takara) for RT-qPCR. A NanoDrop 2000 spectrophotometer was used to determine RNA purity and quantity. The purified RNA was digested with DNase and reverse-transcribed into cDNA using a Reverse Transcriptase Kit (ABclonal Technology, China). The cDNA was quantified by qPCR using SYBR Green premix (Yeasen). The primers are listed in Supplementary Table S2. The mRNA level of the gene of interest was normalized to that of GAPDH.

Immunoblotting

Frozen tissue and cells were lysed using RIPA lysis buffer (Biosharp) containing 1 mM PMSF, protease inhibitor cocktail, and phosphatase inhibitor cocktail for 5 min on ice, sonicated for 1 min, and boiled with SDS-sample buffer. The supernatants were subjected to 8–15% SDS-PAGE and transferred to a 0.2 µm polyvinylidene fluoride (PVDF) membrane (Bio-Rad). The membrane was blocked with 5% skim milk and incubated overnight with the indicated primary antibodies to detect GAPDH(1:1000,abclonal), KLF4(1:1000,proteintech, lot:00127709),PRMT6(1:1000,abclonal, lot:4000001 277),H3R2me2a(1:1000,abclonal, lot:2200240501),M MP9(1:1000,wanleibio), vimentin(1:1000,wanleibio), E-cadherin(1:1000,wanleibio) and N-cadherin(1:1000,wanleibio) in Tris-buffered saline (TBS) supplemented with 0.1% Tween 20 at 4 °C. The membrane was then incubated with horseradish peroxidase (HRP)-labeled IgG secondary antibodies, developed with ECL Chemiluminescence Detection Kit (Biosharp) on a ChemiDoc Imaging System (Bio-Rad, USA). The band intensity was quantified using ImageJ software.

Immunohistochemistry (IHC) and immunofluorescence

For immunohistochemistry (IHC), the tissue wax blocks were sectioned, dewaxed, and hydrated for antigen repair. After blocking for 30 min, the tissues were incubated with primary antibodies at 4 °C overnight, followed by incubation with secondary antibodies at room temperature for 1 h the next day.Subsequently, diaminobenzidine was added for color development and re-stained with hematoxylin & eosin (H&E) staining, and the sections were then sealed.

For immunofluorescence, the cells were cultured in a 12-well plate chamber with cell culture imaging dishes and incubated for 24 h. The dishes were transferred into new plates, and the cells on the slides were fixed using 4% paraformaldehyde (Biosharp) and permeabilized using 0.2% Triton X-100 in PBS at room temperature for 15 min. The cells were incubated overnight with primary antibodies at 4 °C. The cells were then probed with Alexa Fluor-conjugated secondary antibody (Invitrogen), washed, and stained with 1 µg/mL 4,6-diamidino-2-phenylindole (DAPI) for 10 min. The images were obtained using confocal microscopy (ZEISS). Immunohistochemical and immunofluorescence staining quantifications were assessed using ImageJ software.

Chromatin immunoprecipitation (ChIP)

In ChIP assay to detect the enrichment of KLF4 at PRMT6 promoter sites, antibodies FLAG (1:500, abcam) were pre-bound to Protein G Dynabeads (Invitrogen) for 9 h in 4 °C. The cells were cross-linked with 1% formaldehyde and quenched with 0.125 M glycine. The cells were collected, washed, and lysed using lysis buffer A (50 mM Tris pH 8.0, 5 mM EDTA, 1% SDS, 1 mM PMSF, and 1:100 protease inhibitor cocktail). DNA was sheared by sonication, and divided into two same parts. One of the parts was separated as input, the other was immunoprecipitated overnight with antibodies FLAG pre-bound to Protein G Dynabeads. Input was treated with 20 µg Proteinase K at 55 °C for 2 h, reversed at 65 °C overnight and digested with RNase A. The beads were washed, and the eluted DNA/protein complexes were treated with 20 µg Proteinase K at 55 °C for 2 h. The cross-link was reversed at 65 °C overnight. The purified DNA was digested with RNase A and then quantified using qPCR together with input DNA, with specific primers listed in Supplementary Table S3. A cycle threshold (CT) value was obtained for each sample, and duplicate sample values were averaged. The IP signals were normalized to input.

In ChIP assay to detect the enrichment of H3R2ME2a at MMP9, N-cadherin, and vimentin promoter sites, antibodies H3(1:500, proteintech) and H3R2ME2a (1:500,abclonal, lot:2200240501) were pre-bound to the same amount of Protein G Dynabeads (Invitrogen) for 9 h in 4 °C. The cells were cross-linked with 1% formaldehyde and quenched with 0.125 M glycine. The cells were collected, washed, and lysed using lysis buffer A (50 mM Tris pH 8.0, 5 mM EDTA, 1% SDS, 1 mM PMSF, and 1:100 protease inhibitor cocktail). DNA was sheared by sonication, and divided into two same parts. One of the parts was immunoprecipitated overnight with antibodies H3 pre-bound to Protein G Dynabeads, the other was immunoprecipitated overnight with antibodies H3R2ME2a pre-bound to Protein G Dynabeads. The beads were washed, and the eluted DNA/protein complexes were treated with 20 µg Proteinase K at 55 °C for 2 h. The cross-link was reversed at 65 °C overnight. The purified DNA was digested with RNase A and then quantified using qPCR, with specific primers listed in Supplementary Table S3. A cycle threshold (CT) value

Tan *et al. Journal of Translational Medicine*   (2024) 22:922

Page 24 of 25

was obtained for each sample, and duplicate sample values were averaged. The 2-ΔΔCT method was used to calculate relative expression of each target gene. Briefly, mean CT value of the target genes which detected in DNA eluted from Protein G Dynabeads pre-bound with antibodies H3R2ME2a in each sample was normalized to averaged mean CT value of the target genes which detected in DNA eluted from Protein G Dynabeads pre-bound with antibodies H3(ΔCT). This was then normalized to control samples (ΔΔCT), and the 2-ΔΔCT value was obtained [36, 37]. The specific primers listed in Supplementary Table S3.

Subcellular fractionation

Cells were harvested and resuspended in buffer B (10 mM HEPES pH8.0, 10 mM KCl, 1.5 mM MgCl2, 1 mM DTT, 1% Igepal CA-630, 1 mM PMSF, and proteinase inhibitor cocktail). After centrifugation at 16,363 g for 10 min, the supernatant was collected as the cytoplasmic fraction. The pellet was resuspended in 80 μL RIPA lysis buffer (Biosharp) at 4 ℃ for 20 min. After sonication for 1 min, the supernatant was collected as the nuclear fraction.

Statistical analysis

All data were expressed as mean ± standard deviation (SD). Two groups were compared using t-tests, while one-way ANOVA was used to compare multiple groups. $p < 0.05$ indicated statistical significance.

Supplementary Information

The online version contains supplementary material available at https://doi.org/10.1186/s12967-024-05707-5.

Supplementary material 1

Supplementary material 2

Supplementary material 3

Supplementary material 4

Supplementary material 5: Fig. S1. GO and KEGG enrichment analyses，protein interaction network analysis were performed on differentially expressed genes in the villus tissue between NP and URSA. GO enrichment analyses revealed that the NP and the URSA groups differed primarily in interferon release, ERK1/2 signal activation, cell progression, and metabolic processes.KEGG analysis showed that different genes were primarily enriched in the HIF-1a signaling, EGFR, and other signaling pathways.Protein interaction network analysis was performed for differentially expressed genes in Fig

Supplementary material 6: Fig. S2. KLF4 may related to proliferation, invasion, migration, apoptosis and epithelial mesenchymal transformation. Interaction analysis network between KLF4 and the signature proteins of proliferation, invasion, migration, apoptosis and epithelial mesenchymal transformation

---

Author contributions

YL T, JY W and CM L equally contributed to this study. YL T and JY W designed the experiments. CM L collected the specimens and performed the follow-up. SJ W and MQ Z interpreted the results. Y Z, TL Y and J Y conducted the data analysis and interpretation. YL T, JY W, Y Z, TL Y, and J Y wrote the manuscript. All the authors have read and approved the final version of the manuscript.

Data availability

The original contributions presented in the study are included in the article/supplementary material. Further inquiries can be directed to the corresponding authors.

Declarations

Ethics approval and consent to participate

This study included 15 patients who terminated their pregnancies for non-medical reasons (normal pregnancy, NP group) and 12 patients with URSA two or more times (URSA group). The study enrolled patients treated in Renmin Hospital of Wuhan University from October,2021 to January,2023. Patients in the NP group had a history of more than one live birth, with no history of adverse pregnancy, including spontaneous abortion, eclampsia, and preterm birth. URSA patients with the following characteristics were excluded: [1] abnormal anatomical structure of the reproductive tract [2], chromosomal abnormalities in parents or embryos [3], infectious diseases, and [4] endocrine or metabolic diseases. These patients had an abortion between seven and nine weeks of gestation to terminate the unintended pregnancy. All procedures were approved by the Ethics Committee of Renmin Hospital of Wuhan University (No. WDRY2021-K044). Patients with a normal pregnancy and URSA who underwent an induced abortion provided written informed consent. The procedures used in this study adhere to the tenets of the Declaration of Helsinki.

Consent for publication

All authors approved the final manuscript and the submission to this journal.

Competing interests

The authors declare no competing interests.The 8-week-old female and male C57BL/6 mice were kept in a specific pathogen-free (SPF) environment under standard environmental conditions (22–24 ℃ and 60–70% relative humidity). All protocols and experiments of mice were approved by the Animal Care and Use Committee of Wuhan University (Approval number: 20190710).

Author details

[1]Reproductive Medicine Center, Renmin Hospital of Wuhan University, Wuhan, China. [2]Department of Clinical Laboratory, Renmin Hospital of Wuhan University, Wuhan, China. [3]Department of Pediatrics, Zhongnan Hospital of Wuhan University, Wuhan, Hubei, China. [4]Department of Respiratory and Critical Care Medicine, Renmin Hospital of Wuhan University, 430060 Wuhan, China.

References

1. Rai R, Regan L. Recurrent miscarriage. Lancet. 2006;368(9535):601–11.
2. La XL, Wang WJ, Zhang M, Liang L. Definition and multiple factors of recurrent spontaneous abortion. Environ Female Reproductive Health. 2021;1300:231–57.

3. Ibrahaim Y, Hotaling J. Sperm epigenetics and its impact on male fertility, pregnancy loss, and somatic health of future offspring. Sem Reprod Med. 2018;36(3–4):233–5.

4. Adhikari D, Lee IW, Al-Zubaidi U, Liu J, Zhang QH, Yuen WS, et al. Depletion of oocyte dynamin-related protein 1 shows maternal-effect abnormalities in embryonic development. Sci Adv. 2022;8(24):eabl8070.

5. Huppertz B. Traditional and new routes of Trophoblast Invasion and their implications for pregnancy diseases. Int J Mol Sci. 2020;21(1):289.

6. Abbas Y, Turco MY, Burton GJ, Moffett A. Investigation of human trophoblast invasion. Hum Reprod Update. 2020;26(4):501–13.

7. Knöfler M, Haider S, Saleh L, Pollheimer J, Gamage TKJB, James J. Human placenta and trophoblast development: key molecular mechanisms and model systems. Cell Mol Life Sci. 2019;76(18):3479–96.

8. He ZH, He J, Xie KP. KLF4 transcription factor in tumorigenesis. Cell Death Discov. 2023;9(1):118.

9. Wang QZ, Xu J, Chen Y, Liu LM. KLF4 overexpression decreases the viability, invasion and migration of papillary thyroid cancer cells. Exp Ther Med. 2019;18(5):3493–501.

10. Wang XY, Xia SL, Li HC, Wang X, Li CA, Chao YL, et al. vol 27, pg 1747, The deubiquitinase USP10 regulates KLF4 stability and suppresses lung tumorigenesis (2019). Cell Death Differ. 2023;30(10):2364.

11. Audia JE, Campbell RM. Histone Modifications and Cancer. Csh Perspect Biol. 2016;8(4):a019521.

12. Zaib S, Rana N, Khan I. Histone modifications and their role in Epigenetics of Cancer. Curr Med Chem. 2022;29(14):2399–411.

13. Zhang YJ, Sun ZX, Jia JQ, Du TJ, Zhang NC, Tang Y, et al. Overview of histone modification. Histone Mutations Cancer. 2021;1283:1–16.

14. Mobley RJ, Raghu D, Duke LD, Abell-Hart K, Zawistowski JS, Lutz K, et al. MAP3K4 controls the chromatin modifier HDAC6 during trophoblast stem cell epithelial-to-mesenchymal transition. Cell Rep. 2017;18(10):2387–400.

15. Bhattad GJ, Jeyarajah MJ, McGill MG, Dumeaux V, Okae H, Arima T, et al. Histone deacetylase 1 and 2 drive differentiation and fusion of progenitor cells in human placental trophoblasts. Cell Death Dis. 2020;11(5):311.

16. Kwak YT, Muralimanoharan S, Gogate AA, Mendelson CR. Human trophoblast differentiation is associated with profound gene regulatory and epigenetic changes. Endocrinology. 2019;160(9):2189–203.

17. Huang ZY, Du GZ, Huang XM, Han L, Han XM, Xu B, et al. The enhancer RNA lnc-SLC4A1-1 epigenetically regulates unexplained recurrent pregnancy loss (URPL) by activating CXCL8 and NF-kB pathway. Ebiomedicine. 2018;38:162–70.

18. Meister S, Hahn L, Beyer S, Paul C, Mitter S, Kuhn C, et al. Regulation of epigenetic modifications in the placenta during preeclampsia: PPARγ influences H3K4me3 and H3K9ac in extravillous trophoblast cells. Int J Mol Sci. 2021;22(22):12469.

19. Li X, Yang NN, Wu Y, Wang XG, Sun JP, Liu L, et al. Hypoxia regulates fibrosis-related genes via histone lactylation in the placentas of patients with preeclampsia. J Hypertens. 2022;40(6):1189–98.

20. Guccione E, Richard S. The regulation, functions and clinical relevance of arginine methylation (July, 10.1038/S41580-019-0155-X, 2019). Nat Rev Mol Cell Bio. 2019;20(9):567.

21. Grypari IM, Logotheti S, Zolota V, Troncoso P, Efstathiou E, Bravou V, et al. The protein arginine methyltransferases (PRMTs) PRMT1 and CARM1 as candidate epigenetic drivers in prostate cancer progression. Medicine. 2021;100(36):e27094.

22. Chen ZX, Gan JF, Wei Z, Zhang M, Du Y, Xu CJ, et al. The Emerging Role of PRMT6 in Cancer. Front Oncol. 2022;12:841381.

23. Okuno K, Akiyama Y, Shimada S, Nakagawa M, Tanioka T, Inokuchi M, et al. Asymmetric dimethylation at histone H3 arginine 2 by PRMT6 in gastric cancer progression. Carcinogenesis. 2019;40(1):15–26.

24. Qiang LH, Zhang Y, Lei ZH, Lu Z, Tan SS, Ge P, et al. A mycobacterial effector promotes ferroptosis-dependent pathogenicity and dissemination. Nat Commun. 2023;14(1):1430.

25. Quadrini KJ, Bieker JJ. Kruppel-like zinc fingers bind to nuclear import proteins and are required for efficient nuclear localization of erythroid kruppel-like factor. J Biol Chem. 2002;277(35):32243–52.

26. Kamikawa Y, Yasuhara N, Yoneda Y. Cell type-specific transcriptional regulation of the gene encoding importin-α1. Exp Cell Res. 2011;317(14):1970–8.

27. Luo YH, Xie C, Brocker CN, Fan J, Wu X, Feng LJ, et al. Intestinal PPARα protects against colon carcinogenesis via regulation of methyltransferases DNMT1 and PRMT6. Gastroenterology. 2019;157(3):744.

28. Deng TQ, Liao XY, Zhu SM. Recent advances in treatment of recurrent spontaneous abortion. Obstet Gynecol Surv. 2022;77(6):355–66.

29. Cui JJ, Shi M, Quan M, Xie KP. Regulation of EMT by KLF4 in gastrointestinal Cancer. Curr Cancer Drug Tar. 2013;13(9):986–95.

30. Zeng LD, Zhu YM, Moreno CS, Wan Y. New insights into KLFs and SOXs in cancer pathogenesis, stemness, and therapy. Sem Cancer Biol. 2023;90:29–44.

31. Fan WQ, Zhou WB, Yan Q, Peng Y, Wang HY, Kong CC, et al. Upregulation of METTL14 contributes to trophoblast dysfunction by elevating FOXO3a expression in an m A-dependent manner. Placenta. 2022;124:18–27.

32. Li XC, Jin F, Wang BY, Yin XJ, Hong W, Tian FJ. The m6A demethylase ALKBH5 controls trophoblast invasion at the maternal-fetal interface by regulating the stability of mRNA. Theranostics. 2019;9(13):3853–65.

33. Zhang TT, Jiang ZY, Yang NN, Ge ZP, Zuo Q, Huang SY, et al. N6-methyladenosine (m6A) modification in Preeclampsia. Reprod Sci. 2023;30(11):3144–52.

34. Zheng QL, Yang FL, Gana HL, Jin LP. Research paper hypoxia induced ALKBH5 prevents spontaneous abortion by mediating m A-demethylation of SMAD1/5 mRNAs. Bba-Mol Cell Res. 2022;1869(10):119316.

35. Huang HL, Weng HY, Zhou KR, Wu T, Zhao BS, Sun ML, et al. Histone H3 trimethylation at lysine 36 guides m a RNA modification co-transcriptionally. Nature. 2019;567(7748):414–.

36. He F, Yu Q, Wang M, Wang RS, Gong XYJ, Ge F, et al. SESAME-catalyzed H3T11 phosphorylation inhibits Dot1-catalyzed H3K79me3 to regulate autophagy and telomere silencing. Nat Commun. 2022;13(1):7526.

37. Wu YS, Tang LX, Huang H, Yu Q, Hu BC, Wang G, et al. Phosphoglycerate dehydrogenase activates PKM2 to phosphorylate histone H3T11 and attenuate cellular senescence. Nat Commun. 2023;14(1):1323.

Publisher's note